Published in final edited form as:
Neuroscience. 2013 November 12; 252: 302–319. doi:10.1016/j.neuroscience.2013.07.051.

Hydrogen Sulfide Attenuates Neurodegeneration and Neurovascular Dysfunction Induced by Intracerebral Administered Homocysteine in Mice

Pradip K. Kamat, **Anuradha Kalani**, **Srikanth Givvimani**, **PB Sathnur**, **Suresh C. Tyagi**, and **Neetu Tyagi**
Department of Physiology and Biophysics, School of Medicine, University of Louisville, Louisville, KY 40202, and USA

Abstract

High levels of homocysteine (Hcy), known as hyperhomocysteinemia (HHcy) are associated with neurovascular diseases. H_2S, a metabolite of Hcy, has a potent anti-oxidant and anti-inflammatory activity; however, the effect of H_2S has not been explored in Hcy (IC) induced neurodegeneration and neurovascular dysfunction in mice. Therefore, the present study was designed to explore the neuroprotective role of H_2S on Hcy induced neurodegeneration and neurovascular dysfunction. To test this hypothesis we employed wild type (WT) males ages 8–10 weeks, WT+ artificial cerebrospinal fluid (aCSF), WT+ Hcy (0.5μmol/μl) intracerebral injection (I.C., one time only prior to NaHS treatment), WT+Hcy +NaHS (sodium hydrogen sulfide, precursor of H_2S, 30 μmol/kg, body weight). NaHS was injected intra-peritoneally (I.P.) once daily for the period of 7 days after the Hcy (IC) injection. Hcy treatment significantly increased MDA, nitrite level, acetylcholinestrase activity, TNFα, IL1β, GFAP, iNOS, eNOS and decreased glutathione level indicating oxidative-nitrosative stress and neuroinflammation as compared to control and aCSF treated groups. Further, increased expression of NSE, S100B and decreased expression of (PSD95, SAP97) synaptic protein indicated neurodegeneration. Brain sections of Hcy treated mice showed damage in the cortical area and periventricular cells. TUNEL positive cells and Fluro Jade-C staining indicated apoptosis and neurodegeneration. The increased expression of MMP9, MMP2 and decreased expression of TIMP-1, TIMP-2, tight junction proteins (ZO1, Occuldin) in Hcy treated group indicate neurovascular remodeling. Interestingly, NaHS treatment significantly attenuated Hcy induced oxidative stress, memory deficit, neurodegeneration, neuroinflammation and cerebrovascular remodeling. The results indicate that H_2S is effective in providing protection against neurodegeneration and neurovascular dysfunction.

Keywords

Neuroinflammation; Neurodegeneration; H_2S; Cerebrovascular dysfunction

Address for Correspondence: Neetu Tyagi, Ph.D., Department of Physiology and Biophysics, 500 South Preston Street, Health Sciences Center, A-1201, University of Louisville, Louisville, KY 40202; Phone: 502-852-4145, Fax: 502-852-6239, n0tyag01@louisville.edu.

1. Introduction

Homocysteine (Hcy) is a thiol containing excitatory amino acid, which markedly enhances the vulnerability of neurons cells to excitotoxic and oxidative injury (Eikelboom and Hankey, 1999). It has been reported that Hcy changes hippocampus plasticity and synaptic transmission resulting in learning and memory deficits (Christie et al. 2005; Ataie et al., 2010). Elevated plasma Hcy levels known as hyperhomocysteinemia (HHcy) contribute to neuro-degenerative diseases (Obeid et al., 2007; Kalani et al., 2013). These unfavorable vascular effects of Hcy are believed to be caused by the auto-oxidation of Hcy which leads to cellular oxidative stress through the formation of reactive oxygen species (ROS), including superoxide anion and hydrogen peroxide (White et al., 2001; Perna et al., 2003; Yan et al., 2006). Furthermore, a decrease in endothelial nitric oxide (NO) bioavailability plays a critical role in endothelial cell damage and dysfunction (Tyagi et al., 2009). Impairment of endothelial cell (EC) integrity leads to significant tissue damage and inflammatory responses (Mehta and Malik, 2006) and typically occurs during diseases such as hypertension (Lominadze et al., 1998) and stroke (D'Erasmo et al., 1993). In addition, Hcy increased cytokine levels in the brain suggesting that inflammation might also be associated with the neuronal dysfunction observed in hyperhomocystinuric patients (da Cunha et al., 2010). Also, it is important to note that neuro- inflammation is often involved in the dysfunction of the Blood-Brain Barrier (BBB), i.e. loss of the vascular integrity.

The blood-brain barrier (BBB) is a highly organized endothelial barrier which separates the central nervous system (CNS) from peripheral circulation (Zlokovic, 2008). BBB endothelial cells are different from endothelial cells of other vascular units in that they form specific structures on the membranes of adjacent endothelial cells called tight junctions (Abbott et al., 2006). Tight junction proteins (TJ) are essential to the structural integrity of the BBB. The BBB also contains a scaffold protein complex that holds the paracellular membranous structure together. This is formed by a group of cytosolic membrane proteins called the *zonula occludens* (ZO) protein family which includes ZO1 (Stevenson et al., 1986), ZO2 (Jesaitis and Goodenough, 1994), and ZO3 (Haskins et al., 1998). This complex attaches the tight junction proteins to the cytoskeleton structure by cell-to-cell interactions (Fanning et al., 2007). Of the BBB tight junction proteins identified; occludin is the most important membrane component. Occludin contain four transmembrane domains and two extracellular loops (Furuse et al., 1998; Tsukita and Furose, 2000) ZO1 has been associated with oxidant-induced barrier disruption because it serves as an important linker between perijunctional actin and the tight junction proteins occludin (Musch et al., 2006).

The decreased expression of occludin and ZO-1 in extra cellular junctions results in the formation of gaps between the cells with a marked increase in permeability (Patibandla et al., 2009; Tada et al., 2010). The accumulation of toxic free radicals plays an essential role in this BBB disruption through the activation of matrix metalloproteinases (MMPs) (Gasche et al., 1999; Romanic et al., 1998). MMPs are essential for the breakdown of the extracellular matrix (ECM) components within the basement membrane around cerebral blood vessels and neurons. MMPs are synthesized as pre-enzymes, secreted from cells as proenzymes, and activated by other proteases and free radicals in the extracellular compartment (Lee et al., 2005). Among these MMPs, MMP-2 and MMP-9 are the key enzymes (Romanic et al., 1998). Several reports have suggested that MMP-9 plays a significant role in brain injury after cerebral ischemia (Fujimura et al., 1999; Lee et al., 2004). Pharmacological inhibition of MMP-9 as well as targeted deletion of the MMP-9 gene in mice resulted in substantial reductions of brain damage after ischemia (Asahi et al., 2000; Wang et al., 2000). Along with MMPs, the role of tissue inhibitor of metalloproteinase (TIMP) in neuronal degeneration has also been suggested (Alvarez-Sabin et al., 2004). Therefore, preventing Hcy neurotoxicity may be a novel therapeutic strategy

for neurovascular diseases. Interestingly, in addition to cysteine, Hcy metabolites can also produce hydrogen sulfide (H_2S) by cystathionine beta synthase (CBS), cystathionine gamma lyase (CSE) and mercapto sulfur transferase (MST) enzymes (Zhao et al., 2001, Tyagi et al., 2010). The biological and physiological effects and the importance of H_2S in neuro-protection have been extensively reported (Szabo, 2007). The most recent study by our group has demonstrated that H_2S relieved Hcy-induced oxidative stress in brain endothelial cells (Tyagi et al., 2009) as well as reduced HHcy-induced microvascular permeability (Tyagi et al., 2010) suggesting a promising role of H_2S supplementation as a novel strategy to prevent Hcy-induced neurotoxicity.

Therefore, the purpose of the current study was to assess the potential role of H_2S against the neurotoxicity and neurovascular dysfunction induced by Hcy (IC). We demonstrated that Hcy (IC) enhances oxidative stress and neuroinflammation which activates MMPs and de-activates TIMPs. This in turn degrades tight junction proteins causing BBB alteration, memory impairment, and leads to neurovascular dysfunction. The pretreatment with H_2S can prevent these alterations and thus has a neuro-protective property.

2. Material & Methods

2.1. Antibodies and reagents

Homocysteine, NaHS, Acetylthiocholine iodide, D-thiobis nitrobenzoic acid, Thiobarbutric acid, sulphalinamide were purchased from SIGMA-ALDRICH (St. Louis, MO). HRP-conjugated secondary antibodies were purchased from Santa CRUZ BIOTECHNOLOGY (Santa Cruz, CA). Antibodies MMP9, MMP2, NSE, S110B, PSD95, SAP97, ZO1, and Occuldin were purchased from ABCAM (Cambridge, MA). Fluorescent secondary antibodies and primers were procured from INVITROGEN (Carlsbad, CA). Bradford protein assay reagents, PVDF membrane and all other chemicals for analytical grade were purchased from BIO-RAD (Hercules, CA).

2.1.1. Animals—Male (FVB) wild type (8–10 week old) mice were obtained from Jackson Laboratory (Bar Harbor, ME) and kept in the animal care facility in University of Louisville where ambient environmental conditions (12:12-h light-dark cycle, 22–24°C) were maintained. The animals were fed standard food and water ad libitum. All animal procedures were reviewed and approved by the Institutional Animal Care and Use Committee of the University of Louisville, School of Medicine in accord with Animal Care and Use Program Guidelines of the National Institutes of Health.

2.1.2. Drugs-preparation and administration—Hcy powder was dissolved in artificial cerebrospinal fluid (aCSF; 147 mM NaCl, 2.9 mM KCl, 1.6 mM $MgCl_2.6H_2O$, 1.7 mM $CaCl_2$, 2.2 mM dextrose dissolved in distilled water) used as a vehicle for intracerebral administration of Hcy. In the Hcy group, a single administration of Hcy (0.5 μmol/μl) was given intracerebral (IC) in mice brain. Sodium hydrogen sulfide (NaHS, a H_2S donor) was dissolved in 0.9% normal saline. Hcy (I.C) injected mice was treated with NaHS (30μM/kg/day/i.p) for 7 days through intra-peritoneal. NaHS dose was selected on the basis of earlier reports, which have demonstrated its protective effects. Animals of the control group did not receive any intracerebral (IC) injection. Biochemical, behavioral and histo-pathological analyses were done after 24h of the last NaHS or its vehicle injection in the separate groups.

2.1.3. Intracerebral (IC) injection of Hcy—Mice were anesthetized with tribromoethanol (TB; 2.5 gm, 2,2,2 tribromoethanol (TBE); 5 ml 2-methyl-2-butanol (tertiary amyl alcohol) 200 ml distilled water - neutral pH) (200 μg/gm, i.p). A 27-gauge hypodermic needle attached to a 100 μl Hamilton syringe was inserted (2.5 mm depth) perpendicularly through the skull into the brain. Hcy (0.5μm/μl), dissolved in freshly

prepared aCSF, was administered slowly through intracerebral (IC) route. The site of injection was 2 mm from either side of the midline on a line drawn through the anterior base of the ears. We injected Hcy only one side from the midline. The syringe was left in the place for a further 2 min for proper diffusion of Hcy.

2.1.4. Experimental design and drug administration—The mice were grouped as:

Control: Mice injected by intra-peritoneal with vehicle (0.9% normal saline) of NaHS for 7 days.

aCSF: Mice injected by intracerebral (IC) with artificial cerebrospinal fluid (aCSF) once and treated with vehicle for 7 days by intra-peritoneal.

Hcy: Mice injected IC with Hcy (0.5μm/μl) once and treated with vehicle for 7 days by intra-peritoneal.

NaHS (H_2S Donar): NaHS (30μM/kg/day) injected by intra-peritoneal for 7 days in Hcy (0.5μm/μl) treated mice.

2.1.5. Novel object recognition test—Novel object recognition is a validated and widely used test for assessing recognition memory (Lyon et al., 2011). Mice were placed individually in a testing chamber with beige walls for a 5min habituation interval and returned to home cage. Thirty minutes later mice were placed in the testing chamber for 10 min with two identical objects (acquisition session). Mice were returned to home cages and one day later placed back into the testing chamber in the presence of one of the original objects and one novel object (recognition session) for 5 min. The chambers and objects were cleaned with ethanol between trials. Exploratory behavior was defined as sniffing, touching and directing attention to the object. Expected normal behavior would be, with a short delay between Acquisition and Retention trials, that the animal explores the novel object for a longer period of time than the familiar object. A “memory score is calculated for each animal, defined as the time spent in exploring the novel object as a percentage of total time exploring both objects during the retention trial. For the acquisition session, the recognition index (RI) was calculated as (time exploring one of the objects/the time exploring both objects). For the recognition session, the RI was calculated as (time exploring the novel object/the time exploring both the familiar and novel object). Discrimination index was also calculated (DI = (Novel Object Exploration Time/Total Exploration Time)−(Familiar Object Exploration Time/Total Exploration Time) ×100) in mice.

2.1.6. Brain tissue collection and Protein extraction—The mice were sacrificed with anesthesia at the end of memory function test. Brain was removed quickly after intra-cardiac perfusion with chilled normal saline and kept on ice-cold PBS immediately. Whole brains were used for estimation of biochemical and molecular studies. Brain samples from each group were weighed and homogenized in 1× RIPA buffer (Tris–HCl 50 mM, pH 7.4; NP-40, 1%; 0.25% Na-deoxycholate, 150 mM NaCl; 1 mM EDTA; 1 mM PMSF; 1 μg/ml each of aprotinin, leupeptin, pepstatin; 1 mM Na_3VO_4; 1 mM NaF) containing 1 mM PMSF and 1 μg complete protease inhibitor (Sigma). The homogenate was kept on ice for 30 min and centrifuged (100 g) for 10 minutes at 4°C, and then the supernatant was removed and centrifuged a second time (20,000 g for 15 minutes at 4°C) to remove any remaining debris. Protein levels for all samples were quantified by the Bradford method (Bio-Rad, CA) and stored at −80°C for further use.

2.2. Biochemical estimation

2.2.1. Measurement of Malondialdehyde—Malondialdehyde (MDA), a marker of lipid peroxidation, was estimated in the brain tissues, according to the method of Colado et

al. (1997). After homogenization, tissue homogenate was mixed with 30% trichloroacetic acid (TCA), 5 N HCl followed by the addition of 2% thiobarbituric acid (TBA) in 0.5 N NaOH. The mixture was heated for 15 min at 90 °C and centrifuged (Remi cold centrifuge) at 12,000 × g for 10 min. The pink color of the supernatant was measured at 532 nm. MDA concentration was calculated by using standard curve prepared with Tetra ethoxy propane and expressed as nmol/mg protein.

2.2.2. Measurement of Glutathione—Glutathione (GSH) was determined by its reaction with 5,5′-dithiobis (2-nitrobenzoic acid) (DTNB) to yield a yellow chromophore, which was measured spectrophotometrically (Ellman et al., 1959). The brain homogenate was mixed with an equal amount of 5% TCA and centrifuged at 2000 × g for 10 min at 4 °C. The supernatant was collected and further used for reduced GSH estimation. To 0.1 ml of processed tissue sample, 2 ml of phosphate buffer (pH 8.4), 0.5 ml of DTNB and 0.4 ml of double-distilled water were added and the mixture was shaken vigorously on vortex. The absorbance was read at 412 nm. Reduced GSH concentration was calculated by using standard curve prepared with reduced glutathione and expressed as μg/mg protein.

2.2.3. Nitrite estimation—Nitrite was estimated in the mice brain using the Greiss reagent and served as an indicator of nitric oxide (NO) production (Green et al., 1982). 100 μl of Greiss reagent (1:1 solution of 1% sulphanilamide in 5% ortho-phosphoric acid and 0.1% napthaylamine diamine dihydrochloric acid in water) was added to 100 μl of supernatant and absorbance was measured at 542 nm. Nitrite concentration was calculated using a standard curve for sodium nitrite and expressed in μg/mg protein.

2.2.4. Sample preparation and assay of AChE activity—A 10% (w/v) homogenate of brain samples (0.03 M sodium phosphate buffer, pH 7.4) was prepared by using a Teflon homogenizer. The brain homogenate in volume of 200μl was mixed with 1% Triton X-100 (1%, w/v in 0.03 M sodium phosphate buffer, pH 7) and centrifuged at 30,000 rpm at 4°C in a centrifuge for 60 min. Supernatant was collected and stored at 4°C for acetyl cholinesterase estimation by Ellman's method (1959). The kinetic pro le of enzyme activity was measured at 412 nm with an interval of 15 s. One unit of acetyl cholinesterase activity was defined as the number of micromoles of acetylthiocholine iodide hydrolyzed per min/ mg of protein. The specific activity of acetylcholinesterase is expressed in μmol/min/mg protein.

2.2.5. Western blotting—Western blot analysis for oxidative stress, matrix associated proteins and neural damage was performed as follows. Briefly, protein was extracted using 1x RIPA buffer. Equal amount of proteins from brain were fractionated by SDS-PAGE and transferred onto PVDF membrane (BioRad, Hercules, CA) by wet transfer method. Non-specific sites were blocked with 5% non-fat dry milk in TBS-T (50 mM Tris–HCl, 150 mM NaCl, 0.1% Tween- 20, pH 7.4) for 1 h at room temperature following the membrane was washed with washing buffer (pH 7.6, TBS, 0.1% Tween 20) for 3 times,10 min each. The blot was then incubated for overnight at 4°C with appropriate primary antibody in blocking solution according to the supplier's specific instructions. The blots were washed with TBS-T (3 times, 10 min each) and incubated with appropriate HRP- conjugated secondary antibody for 2 h at room temperature. After washing, ECL Plus substrate (Thermo scientific, inc.) was as applied to the blot images were capture in gel documentation system. Relative optical density of protein bands was analyzed using gel software image lab 3.0. The membranes were stripped and re-probed with GAPDH as a loading control.

2.2.6. Reverse transcription polymerase chain reaction (RT-PCR)—The RT-PCR was performed for the expression of ZO1, Occuldin, MMP9, MMP2, TIMP1, TIMP2, iNOS,

eNOS, GFAP, TNFα, IL1β and GAPDH in all experimental group using ImProm-II™ Reverse Transcription system kit (Promega Corporation, Madison, WI, USA). Total RNA was isolated from brain using TRIzol reagent according to the manufacturer instruction. RNA quantification was determined spectrophotometrically by using nanodrop and purity of the RNA was determined by A260/A280. 2 μg of total RNA was reverse transcribed using using ImProm-II™ Reverse Transcription system kit. The reverse transcription program was 25°C for 10 min, 42°C for 50 min, and then 70°C for 15 min. For gene amplification the RT-PCR program was 95°C–7.00 min, [95°C–50 sec, 55°C–1.00 min, 72°C–1.00 min]x34 cycle, 72°C–5.00 min, 4°C-∞. The primers for RT-PCR are obtained from Invitrogen (carlsbad, CA) and described in Table 1. The RT-PCR product was electrophoresed on 1.5% agarose gel in TAE with 0.008% ethidium bromide.

2.2.7. Preparation of Barium sulphate—Barium sulphate has been widely used by the radiologists in to visualize the structural and motility abnormalities of blood vessel vasculature. Barium sulphate was dissolved in 50 mM Tris-buffer (pH 5.0) and infused slowly at a constant flow and pressure with a syringe pump using carotid artery (Myojin et al., 2007; Givvimani et al., 2011). This produced the optimal visualization of vascular density in brain. Animals were dissected open to expose and brain angiograms were performed in Kodak 4000 MM image station.

2.2.8. Angiography—Brain angiogram is an imaging test that uses X-rays to view brain blood vessels. Dissected animals were placed in the X-ray chamber and angiograms were captured with high penetrative phosphorous screen by 31 KVP X-ray exposures for 3 minutes. It is often use this test to study narrow, blocked, enlarged, or malformed arteries or veins in many parts of body, including brain.

2.2.9. Cryo-sectioning—After euthanizing the mice, brain tissue was harvested and washed thoroughly in phosphate buffered saline (PBS) and preserved in a Peel-A-Way disposable plastic tissue embedding molds (Polysciences inc., Warrington, PA., USA) having tissue freezing media (Triangle Biomedical Sciences, Durham, N.C., USA) at −80° C until further use. 25 μm and 10 μm thick tissue sections were made using cryotome (Leica CM 1850) and placed on super frost plus microscope slides, air-dried and processed for staining.

2.3. Histological Study

2.3.1. Hematoxylin and Eosin (HE) staining—A histopathological study was conducted in brain tissue by chromophore kit (Rechard Allan scientific, USA) according to manufacturer instruction. Mice were anesthetized under ether anesthesia. The transcardial perfusion with 5 ml of phosphate-buffered saline (0.02 M, pH 7.4), followed by 5 ml of 4% paraformaldehyde in 0.1 M phosphate-buffered saline (pH 7.4) was done for pre-fixation of the brain tissue. Then, the brain was dissected out carefully and was kept in 4% paraformaldehyde overnight at room temp for post fixation. After post-fixation, the tissue was kept in 30% sucrose for 24 h. Block was prepared in tissue freezing media and coronal sections (10 μm) were cut with the help of a cryotome (Leica instrument, USA) and picked up on poly-L-lysine coated slides. Sections from the rostral to the caudal portion of the brain were stained with hematoxylin and eosin (Li et al., 1998). Stained sections were captured (light microscopy) at 60x magnification. Dead cells were identified morphologically by blebbing of plasma membrane, diffused pallor of eosinophilic background, alterations in size and shape of cells, vacuolation and condensed nucleus.

2.3.2. Terminal deoxynucleotidyl transferase-mediated, dUTP nick end labelling (TUNEL)—TUNEL staining was conducted on frozen brain section from all

groups using a commercially available kit (Dead End Fluorometric TUNEL System; Promega). Staining was done according to manufacturer's instructions keeping positive and negative controls.

2.3.3. Fluro Jade-C (FJC) staining—FJC labelling in the brain section was performed using a standard protocol (Schmued et al., 2005), with modification, as follows: (a) sections were deparaffinised by two 5 min washes in xylene, rehydrated through a graduated alcohol series, and washed for 2 min in distilled water; (b) sections were transferred to 0.06% potassium permanganate solution for 10 min, then rinsed in distilled water for 2 min; (c) sections were incubated for 20 min in a 0.0001% solution of FJC (Sigma Aldrich, USA). FJC was made immediately before use by diluting a stock solution of 0.01% FJC by 100-fold in 0.1% acetic acid; (d) sections were washed 3 times for 1 min in distilled water, dried at 37 °C and mounted with DPX; and the fluorescent signal visualized using a confocal laser-scanning microscope with an excitation wavelength of 488 nm.

2.4. Statistical analysis

The results are expressed as mean ± S.E.M. Statistical analysis of the biochemical, molecular data and novel object recognition test were done by one-way analysis of variance (ANOVA) followed by Tukey test. A *p value <0.05* was considered to be significant.

3.0. Results

3.1.1. Memory function: Effect of NaHS on Hcy induced memory impairment—The novel object recognition test was performed for memory function in mice. We tested WT mice treated with in a novel object recognition task that relies on the mouse's natural exploratory behavior shows the schematic representation of the protocol, in which mice are habituated to the open-field apparatus, on day 1 they were allowed to explore two identical objects, and after 24 hours, they were presented with the familiar and a new object. Hcy (IC) treated mice exhibit significantly impaired novel object recognition performance in the simple task relative to wild type mice exploring the novel object. There was no any change in recognition index (RI) in acquisition trial [$F(3, 16)=5.23$; $P>0.05$] among the group but significant change were observed in retention trial [$F(3, 16)=5.23$; $P<0.05$]. Consistent with the lack of net preference between novel and familiar objects, the discrimination index in Hcy treated mice was reduced [$F(3, 16)=3.13$; $P<0.05$] with respect to wild types. NaHS treatment led to improved preference between novel and familiar object in Hcy treated mice [$F(3, 16)=2.71$; $P<0.05$] (Fig. 1A, 1B and 1C).

3.1.2 Effect of NaHS on Hcy induced oxidative stress and AChE activity—To evaluate the neuro-protective effects of NaHS on Hcy induced brain redox status. Several important indices about oxidative stress in brain were determined. As an index of oxidative stress, the level of lipid peroxidation product, MDA, was significantly increased in Hcy treated group as compared to control and aCSF groups. This increase in MDA was attenuated by NaHS treatment; however administration of aCSF had no significant effect on MDA level as compared to control (Fig. 2A). As shown in Fig. 2B the concentration of reduced GSH was markedly decreased in the Hcy treated group as compared to control and aCSF groups. Treatment with NaHS normalized the decreased levels of reduced GSH in Hcy treated group. In addition, Hcy treatment also caused a significant increase the acetylcholinesterase (AChE) activity (μmol/min/mg protein) when compared with control and aCSF treated mice. NaHS treatment was unable to prevent increased in AChE activity as shown in Fig. 2C. These findings suggest that treatment with NaHS could reduce redox homeostasis of brain (Fig. 2)

3.1.3. Effect of NaHS on Hcy induced neuroinflammatory markers (TNFα and of IL-1β) and astrocyte marker (GFAP)—Neuroinflammation is reflected in cerebro-vascular dysfunction by astrogliosis and microglial activation. A significant increase in mRNA and protein expression of GFAP was observed in Hcy treated group as compared to aCSF and control groups (Fig. 3). Remarkably NaHS treatment significantly decrease the mRNA and protein expression of GAFP in Hcy treated mice brain as shown in Fig. 3A, B, C and D. We also quantified mRNA and protein expression for the pro-inflammatory cytokines IL-1β and TNFα. There was increased expression of TNFα and IL-1β mRNA and protein in Hcy treated mice as compared to aCSF and control group (Fig. 3E, F, G, H, I and J). NaHS treatment restored TNFα and IL-1β mRNA and protein expression in Hcy treated group (Fig. 3E, F and G). These results suggest the anti-inflammatory action of NaHS (Fig. 3).

3.1.4. Effect of NaHS on Nitic oxide synthase (iNOS and eNOS) and nitrite level—To elucidate the effect of Hcy on NO bio-availability, we measured iNOS and eNOS mRNA and protein levels. As shown in Fig. 4, a significant increase in mRNA and protein expression of iNOS and eNOS were observed in Hcy treated group as compared to aCSF and control groups. Interestingly, NaHS showed a significant decrease in iNOS and eNOS protein as well as mRNA levels. We also measured NO metabolite nitrite levels in brain. As shown in Fig. 4E, nitrite levels were significantly elevated in Hcy treated group compared to control and aCSF treated groups. Treatment with NaHS significantly restored nitrite levels. Morover, the nitrite level was not significantly altered in aCSF treated group as compared to control (Fig. 4).

3.1.5. Effect of NaHS on Hcy induced neuronal injury and synaptic markers—S100B, NSE, PSD95 and SAP97 protein level was investigated by Western Blot analysis. There was increased protein expression of SB100B and NSE in Hcy treated group as compared to aCSF and control group (Fig. 5). However PSD95 and SAP97 protein expression was decreased in Hcy treated group as compared to aCSF and control group (Fig. 6). Further, NaHS treatment significantly recovered Hcy induced changes in synaptic markers (Fig. 5 & 6).

3.2. Histopathological observations: Effect of NaHS on Hcy induced neurodegeneration

3.2.1. HE staining—Histological examination of the brain sections by hematoxylin and eosin staining suggests gross histological variation in Hcy treated mice as compared with other group. Hcy treated group showed significant degeneration of cellular constituents indicated by decrease in cell size (shrinkage) and cell number. Hcy administration caused damage to neuron in brain periventricular cortex as well as in hippocampal regions indicates neuro-degeneration in Hcy treated mice brain as compared to control and aCSF treated mice brain (Fig. 7A–D). However, NaHS treatment significantly restored this alteration (Fig. 7E–H).

3.2.2. Tunel staining: NaHS treatment prevents apoptosis—Apoptosis or cell death during HHcy was assessed by Tunel assay. There was significantly increased in apoptosis in Hcy treated group. Treatment with NaHS inhibited the increase in apoptosis in Hcy treated group (Fig. 8). These findings suggest the beneficial role of NaHS in preventing apoptosis.

3.2.3. Fluoro Jade C staining: NaHS inhibits Hcy induced neuronal degeneration—To further examine the neuroprotective effect of NaHS after Hcy induced neurotoxicity, we stained sections of mouse brain with Fluoro Jade C (FJC), a fluorochrome that binds specifically to degenerating fibers and cell bodies of neurons. Results of a typical

experiment are shown in Fig. 9. A large number of FJC-positive cells were observed in brain section of Hcy treated group as compared to control and aCSF groups. There was a significant decrease in the number of FJC-positive cells in the NaHS treated group.

3.2.4. NaHS regulates extra cellular matrix remodeling by altering MMP/TIMP expressions: The proteins involved in vascular function—To assess the role of NaHS on MMPs/TIMPs expression, we determined MMP-2,-9, TIMP-1 and TIMP-2 expression by using Western Blot and RT-PCR. There was an increased mRNA and protein expression of MMP-9 and MMP-2 in Hcy treated group compared to control (Fig. 10A–G). Treatment with NaHS decreased the expression of MMP-9 and MMP-2 (Fig. 10). In contrast, TIMP-1/TIMP-2 mRNA and protein expression showed decrease in Hcy treated group as compared to control which was ameliorated by NaHS treatment (Fig. 11. A–F). These findings suggested NaHS protects cerebro-vascular remodeling by altering the MMP/TIMP axis during neuro-degeneration induced by Hcy. Previously, we and others have shown the association of MMP-9 with degradation of a TJP. Hence, we investigated the role of NaHS in TJP degradation through RT-PCR and Western Blot analysis. There was significantly decreased in mRNA/protein expression of ZO-1, and occuldin proteins in Hcy treated group compared to control groups (Fig. 12A–G). This alteration in TJPs expression was mitigated by NaHS treatment (Fig. 12).

3.3. Effect of NaHS on microvasculature in the brain

The barium X-ray data showed loss of major vessel in Hcy treated group as compared to control and aCSF groups. Exogenous NaHS treatment improved the BBB-microvasculature integrity (Fig. 13.)

4. Discussion

Previously, we showed the novel role of H_2S in HHcy induced cerebral vascular injury (Tyagi et al., 2010). The results of the present study aimed to clarify the neuro-protective effect of H_2S against the neurotoxic effect of Hcy in the brain, which may be one of the mechanisms leading to cerebral vascular injury (Tyagi et al., 2010). Herein, we demonstrated that an IC injection of Hcy triggered oxidative stress and neuro-inflammation leading to a dis-balance of the MMP/TIMP ratio, in part by increasing nitrite levels and degrading the tight junction proteins. This alteration disrupts BBB integrity which causes vascular dysfunction and neurotoxicity and subsequently leads to memory impairment in mice. While H_2S supplementation diminished these effects of Hcy, the data indicates that H_2S specifically inhibits Hcy's effect by reducing the redox stress as well as inflammation.

The brain has a complex pathophysiological process involving many factors, such as oxidative-stress-related free radical species and pro-inflammatory cytokines (Lucas et al., 2006). Oxidative stress is one of the more important events in cerebrovascular disease such as stroke, Parkinson and AD pathology (Uttara et al., 2009). Earlier studies showed lipid peroxidation that is related to neurodegenerative disorder and degeneration of the neuronal membrane (Williams et al., 2006, Petursdottir et al., 2007; Kamat et al., 2010). In agreement with above findings, we also observed elevated levels of MDA in the Hcy administered group as compared to control and CSF treated groups which suggests neuro-degeneration during HHcy. We also found decreased glutathione levels (GSH), which is an antioxidant and principal intracellular non-protein thiol which is known to play a major role in the maintenance of the intracellular redox state. Therefore, in the present study we observed that Hcy caused a significant increase in MDA levels along with a decrease in GSH levels indicating oxidative stress induced by Hcy. Importantly, treatment with NaHS greatly inhibited the formation of MDA levels and significantly increased the levels of GSH (Fig. 2a, 2b). The significantly lower levels of free radical scavengers and the higher level of GSH

promoted by H_2S should induce a protective effect by increasing the metabolism of superoxide and the level of cysteine transport (Kimura et al., 2004; Rossoni et al., 2007). It is earlier reported that there is a close association of neuroinflammation with the pathogenesis of several neurovascular-associated disorders such as: Parkinson's disease (PD), Alzheimer's diseases (AD) and cerebral stroke (Mrak and Griffin, 2001). The activated microglia release pro-inflammatory cytokines, such as tumor necrosis factor-alpha (TNF-α) and interleukin-beta (IL1-β), that trigger neuronal damage and serve as mediators of neuroinflammation (Liu et al., 2003; Rai et al., 2012). We found that the administration of Hcy increased GFAP expression (marker of astrocyte) as compared to control and aCSF groups indicating astrocyte activation during HHcy. Along with astrocyte activation we also observed increased expression of pro-inflammatory cytokines TNFα and IL-1β which is indicative of neuro-inflammation during HHcy. Interestingly, treatment with NaHS significantly decreased expression of GFAP, TNFα and IL-1β. This indicates that the endogenous production of H_2S does have positive anti-inflammatory effects (Fig. 3).

The iNOS expressing microglia are consistently found in case of neurodegenerative diseases and has been reported as a key mediator of glial induced neuronal death (Singh et al., 2011). Endothelial nitric oxide synthase (eNOS) plays an important role in vascular permeability, leukocyte extravasation and angiogenesis. Brain eNOS induce the dilation of blood vessels to promote migration of leukocytes, typically neutrophils, to the area of injury (Duffield, 2003). NO is produced by activated astrocytes, is overexpressed during neuroinflammatory process and is one of the major contributors to the formation of reactive nitrogen species(Min et al., 2009; Calabrese et al., 2000). Some studies have shown that high concentrations of Hcy increased NO production (Kanani et al., 1999) whereas other studies confirmed that Hcy decreased NO production (Weiss et al., 2013). Our present results determined that Hcy increased mRNA and protein levels of iNOS/eNOS and total nitrite, indicating nitrosative stress in Hcy treated group as compared to control and aCSF groups (Fig. 4). Further the nitrosative stress and neuroinflammatory effects induced by Hcy were reduced by NaHS treatments (Fig. 4). These results suggest increased endothelial dysfunction and disturbances of vascular function in Hcy treated group as compared to control and aCSF groups. These results coincided with the earlier reports that H_2S behave as a cerebrovascular dilator (Zhao et al, 2001). S100B and NSE levels have been considered markers of neurodegeneration and are thought to be related to the severity of the disease (Mecocci et al., 1995; Parnetti et al., 1995). Present results illustrated high levels of S100 B and NSE protein expressions in Hcy treated groups as compared to control and aCSF groups. Hcy-induced expression of S100B and NSE drastically decreased with NaHS (H_2S donor) treatment (Fig. 5). These results suggest severe neurodegeneration in Hcy treated brains.

Apoptosis has been considered as one of the main features of neuronal loss that propagates neurodegeneration (Kamat et al., 2011). Here we show an increase in apoptosis by Tunel assay in Hcy treated group as compared to control and aCSF groups (Fig. 8). Treatment with NaHS significantly decreased cell death, thus inhibiting neuronal degeneration. In addition, FJC staining demonstrated that the number of degenerative neurons in the Hcy treated animals was significantly higher than that of the NaHS group (Fig. 9). These data sets indicate that exogenous NaHS could protect the integrity and function of neurons and ultimately reduce the degree of neuronal degeneration. The effect of NaHS was also seen by histopathological changes in brain areas of Hcy treated groups. The histopathological changes were examined by using HE stain in sequential brain sections to confirm the extent of damage. Brain sections of Hcy-treated mice, stained by HE staining, showed increased vacuoles in the cortical area, damaged periventricular cells, and a general disorganization of the hippocampus as compared to control and aCSF treated groups. Hcy caused severe damage to the periventricular cortex. In the periventricular cortex of Hcy-treated mice,

sponginess can be seen clearly but NaHS treatment noticeably prevents the damage to some extent. In the hippocampal regions the extent of damage was found similar to the periventricular cortical region in Hcy treated groups and at this level, NaHS treatment returned cell morphology more closely to that of the control and aCSF treatment groups (Fig. 7).

Synaptic proteins such as synaptosome associated protein-97 (SAP97) and post-synaptic density-95 (PSD-95) are neuronal proteins that are linked with receptors and cytoskeletal elements at synapses and are also involved with the proper development of glutamatergic synapses (El-husseini et al., 2000). Changes in these synaptic markers have been implemented to check neuronal damage (Harigaya et al., 1996). Rao et al. (2011) reported that increased neuroinflammatory cascade leads to loss of synaptic marker protein. With their findings, we also confirmed decreased PSD-95 and SAP-97 protein expressions in Hcy treated group as compared to control and aCSF groups indicating synaptic dysfunction, neuronal damage and disturbance in synaptic plasticity. However these negative effects were mitgated with NaHS treatment (Fig. 6). The cholinergic system has been known to play an important role in memory formation and retrieval. Impaired cholinergic functions are associated with memory impairment (Tota et al., 2012, Kamat et al., 2012). In our study, we found increased AChE activity in Hcy treated groups as compared to control and aCSF groups (Fig. 2c). However, treatment with NaHS was unable to prevent AChE activity in the Hcy treated group.

Previously, we showed that Hcy increased MMP-2/MMP-9 expression in HHcy mouse brains as well as in their brain endothelial cells (Tyagi et al., 2009, Tyagi et al., 2010). However, the role of H_2S in activation of MMPs during neuro-degeneration was not defined. In the present study, for the first time, we demonstrated a significant increase in the MMP-2 and MMP-9 protein as well as mRNA expression in the Hcy treated group mice (Fig. 10). Interestingly, MMP-2, -9 expressions were suppressed with NaHS in Hcy treated group. Li et al. (2009) have suggested that endogenous H_2S may decrease the level of MMP-13 and TIMP-1 in rats. Thus, the balance between MMPs and TIMPs is critical for proper ECM remodeling and is essential for several developmental and morphogenetic processes (Dollery et al., 1999). The mRNA expression level of TIMP-1,-2 significantly decreased in Hcy treated group as compared to control and aCSF groups (Fig. 11). The treatment of NaHS inhibited the HHcy-induced sub-endothelial matrix remodeling, suggesting the protective role of H_2S in cerebral vascular remodeling/injury. The present study, along with earlier reports, suggested a substantial increase in MMP-2 and MMP-9 with increased or decreased expression of their inhibitors (TIMP-1, TIMP-2) (Refsum et al., 1998). The increased MMP-2, -9 protein/mRNA levels caused degradation of TJP and led to an increase in BBB permeability. TJPs play important role in tissue integrity but also in vascular permeability, leukocyte extravasation and angiogenesis (Tyagi et al., 2006). To investigate the BBB integrity we studied the TJ markers ZO-1 and occludin. There was a marked decrease in the expression of ZO-1 and occludin in Hcy treated group as compared to control and aCSF groups. Further, exogenous NaHS treatment restored TJP (ZO-1, and occludin) levels (Fig. 12). These results suggest H_2S reversed the effect of Hcy on cerebral vascular injury, in part, by inhibiting MMPs/TIMP and thus preventing TJP degradation preserving vascular integrity.

Capillary changes, neurovascular dysfunction, and cognitive impairments are features of aging and are related to cerebral stroke and AD (Girouard and Iadecola, 2006). To confirm the status of microvasculature in the brain, we performed angiography by the barium angiogram method. We found that Hcy administration in mice brains leads to a marked loss of major vessels with small collaterals which designate disturbances in BBB integrity as compared to the control and aCSF groups. Importantly, NaHS treatment mitigates Hcy

induced loss of major vessel (Fig. 13). These disturbances in the BBB have been known to contribute to the onset and progression of neurodegenerative diseases including AD, cerebral stroke and vascular dementia (VaD) (Takechi et al., 2012). Our observation defined the novel role of H_2S against Hcy-induced neurodegenration and supported the hypothesis presented in Fig. 14.

In summary, we have shown that intracranial injection of Hcy induced vascular dysfunction, memory impairments, and pathological conditions that are similar to those found in human cerebral stroke and AD. We found Hcy plays a significant role in oxidative stress, neuroinflammation, TJPs, neurodegeneration, apoptosis and MMPs which mutually summate to cause neurovascular dysfunction and ultimately cognitive decline. H_2S supplementation however, showed the reversal effect. Thus, our findings suggest that H_2S could be a beneficial therapeutic candidate for the treatment of HHcy-associated pathologies such as cerebral stroke and neurodegenerative disorders.

Acknowledgments

This work was supported by National Institutes of Health grants HL107640-NT and NS-051568 to SCT.

Abbreviations

BBB	Blood-brain barrier
CNS	Central nervous system
ECM	Extracellular matrix
GFAP	Glial fibrillary acidic protein
IL	Interleukin
MMP	Matrix metalloproteinases
TIMP	Tissue inhibitor of metalloproteinases
TNF	Tumor necrosis factor
nNOS	Neuronal nitric oxide synthase
iNOS	Inducible nitric oxide synthase
eNOS	endothelial nitric oxide synthase
Hcy	Homocysteine
CBS	Cysteine beta synthase
ZO	Zona occuldin
MDA	Melondialdehyde
GSH	Glutathione

References

1. Abbott NJ, Patabendige AA, Dolman DE, Yusof SR, Begley DJ. Structure and function of the blood-brain barrier. Neurobiol Dis. 2010; 37:13–25. [PubMed: 19664713]
2. Abbott NJ, Rönnbäck L, Hansson E. Astrocyte-endothelial interactions at the blood-brain barrier. Nat Rev Neurosci. 2006; 7:41–53. [PubMed: 16371949]
3. Alvarez B, Ruiz C, Chacon P, Alvarez-Sabin J, Matas M. Serum values of metalloproteinase-2 and metalloproteinase-9 as related to unstable plaque and inflammatory cells in patients with greater than 70% carotid artery stenosis. J Vasc Surg. 2004; 40:469–475. [PubMed: 15337875]

4. Asahi M, Asahi K, Jung JC, del Zoppo GJ, Fini ME, Lo EH. Role for matrix metalloproteinase 9 after focal cerebral ischemia: effects of gene knockout and enzyme inhibition with BB-94. J Cereb Blood Flow Metab. 2000; 20:1681–1689. [PubMed: 11129784]
5. Ataie A, Sabetkasaei M, Haghparast A, Moghaddam AH, Ataee R, Moghaddam SN. Curcumin exerts neuroprotective effects against homocysteine intracerebroventricular injection-induced cognitive impairment and oxidative stress in rat brain. J Med Food. 2010; 13:821–826. [PubMed: 20553189]
6. Calabrese V, Copani A, Testa D, Ravagna A, Spadaro F, Tendi E, Nicoletti VG, Giuffrida Stella AM. Nitric oxide synthase induction in astroglial cell cultures: effect on heat shock protein 70 synthesis and oxidant/antioxidant balance. J Neurosci Res. 2000; 60:613–622. [PubMed: 10820432]
7. Christie LA, Riedel G, Algaidi SA, Whalley LJ, Platt B. Enhanced hippocampal long-term potentiation in rats after chronic exposure to homocysteine. Neuroscience letters. 2005; 373:119–124. [PubMed: 15567565]
8. Colado MI, O'Shea E, Granados R, Murray TK, Green AR. In vivo evidence for free radical involvement in the degeneration of rat brain 5-HT following administration of MDMA ('ecstasy') and p-chloroamphetamine but not the degeneration following fenfluramine. Br J Pharmacol. 1997; 121:889–900. [PubMed: 9222545]
9. da Cunha AA, Ferreira AG, Wyse AT. Increased inflammatory markers in brain and blood of rats subjected to acute homocysteine administration. Metab Brain Dis. 2010; 25:199–206. [PubMed: 20424906]
10. D'Erasmo E, Acca M, Pisani D, Volpe MS. Neurological state, infarct size and clinical outcome are related to early platelet count decrease in stroke. Gerontology. 1993; 39:276–279. [PubMed: 8314094]
11. Dollery CM, Humphries SE, McClelland A, Latchman DS, McEwan JR. Expression of tissue inhibitor of matrix metalloproteinases 1 by use of an adenoviral vector inhibits smooth muscle cell migration and reduces neointimal hyperplasia in the rat model of vascular balloon injury. Circulation. 1999; 99:3199–3205. [PubMed: 10377085]
12. Duffield JS. The inflammatory macrophage: a story of Jekyll and Hyde. Clin Sci (Lond). 2003; 104:27–38. [PubMed: 12519085]
13. Eikelboom JW, Lonn E, Genest J Jr, Hankey G, Yusuf S. Homocyst(e)ine and cardiovascular disease: a critical review of the epidemiologic evidence. Ann Intern Med. 1999; 131:363–375. [PubMed: 10475890]
14. El-Husseini AE, Schnell E, Chetkovich DM, Nicoll RA, Bredt DS. PSD-95 involvement in maturation of excitatory synapses. Science (New York, NY. 2000; 290:1364–1368.
15. Ellman GL. Tissue sulfhydryl groups. Archives of biochemistry and biophysics. 1959; 82:70–77. [PubMed: 13650640]
16. Fanning AS, Jameson BJ, Jesaitis LA, Anderson JM. The tight junction protein ZO-1 establishes a link between the transmembrane protein occludin and the actin cytoskeleton. The Journal of biological chemistry. 1998; 273:29745–29753. [PubMed: 9792688]
17. Fanning AS, Little BP, Rahner C, Utepbergenov D, Walther Z, Anderson JM. The unique-5 and -6 motifs of ZO1 regulate tight junction strand localization and scaffold properties. Mol Biol Cell. 2007; 18:721–731. [PubMed: 17182847]
18. Fujimura M, Morita-Fujimura Y, Kawase M, Chan PH. Early decrease of apurinic/apyrimidinic endonuclease expression after transient focal cerebral ischemia in mice. J Cereb Blood Flow Metab. 1999; 19:495–501. [PubMed: 10326716]
19. Furuse M, Fujita K, Hiragi T, Fujimoto K, Tsukita S. Claudin-1 and -2: novel integral membrane proteins localizing at tight junctions with no sequence similarity to occluding. J Cell Biol. 1998; 141:1539–1550. [PubMed: 9647647]
20. Gasche Y, Fujimura M, Morita-Fujimura Y, Copin JC, Kawase M, Massengale J, Chan PH. Early appearance of activated matrix metalloproteinase-9 after focal cerebral ischemia in mice: a possible role in blood-brain barrier dysfunction. J Cereb Blood Flow Metab. 1999; 19:1020–1028. [PubMed: 10478654]
21. Girouard H, Iadecola C. Neurovascular coupling in the normal brain and in hypertension, stroke, and Alzheimer disease. J Appl Physiol. 2006; 100:328–335. [PubMed: 16357086]

22. Givvimani S, Munjal C, Tyagi N, Sen U, Metreveli N, Tyagi SC. Mitochondrial division/ mitophagy inhibitor (Mdivi) ameliorates pressure overload induced heart failure. PloS one. 2012; 7:e32388. [PubMed: 22479323]
23. Givvimani S, Sen U, Tyagi N, Munjal C, Tyagi SC. X-ray imaging of differential vascular density in MMP-9−/−, PAR-1−/+, hyperhomocysteinemic (CBS−/+) and diabetic (Ins2−/+) mice. Archives of physiology and biochemistry. 2011; 117:1–7. [PubMed: 20839901]
24. Green LC, Wagner DA, Glogowski J, Skipper PL, Wishnok JS, Tannenbaum SR. Analysis of nitrate, nitrite, and [15N]nitrate in biological fluids. Anal Biochem. 1982; 126:131–138. [PubMed: 7181105]
25. Harigaya Y, Shoji M, Shirao T, Hirai S. Disappearance of actin-binding protein, drebrin, from hippocampal synapses in Alzheimer's disease. J Neurosci Res. 1996; 43:87–92. [PubMed: 8838578]
26. Haskins J, Gu L, Wittchen ES, Hibbard J, Stevenson BR. ZO-3, a novel member of the MAGUK protein family found at the tight junction, interacts with ZO1 and occludin. J Cell Biol. 1998; 141:199–208. [PubMed: 9531559]
27. Jesaitis LA, Goodenough DA. Molecular characterization and tissue distribution of ZO-2, a tight junction protein homologous to ZO1 and the Drosophila discs-large tumor suppressor protein. J Cell Biol. 1994; 124:949–962. [PubMed: 8132716]
28. Kalani A, Kamat PK, Tyagi SC, Tyagi N. Synergy of Homocysteine, MicroRNA, and Epigenetics: A Novel Therapeutic Approach for Stroke. Mol Neurobiol. 2013
29. Kamat PK, Tota S, Rai S, Shukla R, Ali S, Najmi AK, Nath C. Okadaic acid induced neurotoxicity leads to central cholinergic dysfunction in rats. Eur J Pharmacol. 2012; 690:90–98. [PubMed: 22749976]
30. Kamat PK, Tota S, Saxena G, Shukla R, Nath C. Okadaic acid (ICV) induced memory impairment in rats: a suitable experimental model to test anti-dementia activity. Brain research. 2010; 1309:66–74. [PubMed: 19883632]
31. Kamat PK, Tota S, Shukla R, Ali S, Najmi AK, Nath C. Mitochondrial dysfunction: a crucial event in okadaic acid (ICV) induced memory impairment and apoptotic cell death in rat brain. Pharmacology, biochemistry, and behavior. 2011; 100:311–319.
32. Kanani PM, Sinkey CA, Browning RL, Allaman M, Knapp HR, Haynes WG. Role of oxidant stress in endothelial dysfunction produced by experimental hyperhomocyst(e)inemia in humans. Circulation. 1999; 100:1161–1168. [PubMed: 10484535]
33. Kimura Y, Kimura H. Hydrogen sulfide protects neurons from oxidative stress. FASEB J. 2004; 18:1165–7. [PubMed: 15155563]
34. Lee GA, Lin C-H, Jiang H-H, Chao H-J, Wu C-L, Hsueh C-M. Microglia-derived glial cell line-derived neurotrophic factor could protect Sprague-Dawley rat astrocyte from in vitro ischemia-induced damage. Neuroscience letters. 2004; 356:111–114. [PubMed: 14746876]
35. Lee S-R, Tsuji K, Lee S-R, Lo EH. Role of matrix metalloproteinases in delayed neuronal damage after transient global cerebral ischemia. The Journal of neuroscience: the official journal of the Society for Neuroscience. 2004; 24:671–678. [PubMed: 14736853]
36. Lee SW, Song KE, Shin DS, Ahn SM, Ha ES, Kim DJ, Nam MS, Lee KW. Alterations in peripheral blood levels of TIMP-1, MMP-2, and MMP-9 in patients with type-2 diabetes. Diabetes Res Clin Pract. 2005; 69:175–179. [PubMed: 16005367]
37. Li L, Sun J, Wang C, Wang L, Hovart M, Sheil AG. Graft histology and lymphocyte apoptosis in pancreas allografts combined with liver allografts. Transplant Proc. 1998; 30:2956–2957. [PubMed: 9838304]
38. Liu C, Zhou XS, Geng QM. Evaluation oxygen free radicals related index before liver transplantation to forejudge prognosis. Zhongguo Wei Zhong Bing Ji Jiu Yi Xue. 2003; 15:560–562. [PubMed: 12971857]
39. Lominadze D, Joshua IG, Schuschke DA. Increased erythrocyte aggregation in spontaneously hypertensive rats. Am J Hypertens. 1998; 11:784–789. [PubMed: 9683038]
40. Lucas SM, Rothwell NJ, Gibson RM. The role of inflammation in CNS injury and disease. Br J Pharmacol. 2006; 147(Suppl 1):S232–240. [PubMed: 16402109]

41. Lyon DR, Gunzelmann GM. Functional equivalence and spatial path memory. Q J Exp Psychol (Hove). 2011; 64:2081–2087. [PubMed: 22044400]
42. Mecocci P, Parnetti L, Romano G, Scarelli A, Chionne F, Cecchetti R, Polidori MC, Palumbo B, Cherubini A, Senin U. Serum anti-GFAP and anti-S100 autoantibodies in brain aging, Alzheimer's disease and vascular dementia. Journal of neuroimmunology. 1995; 57:165–170. [PubMed: 7706432]
43. Mehta D, Malik A. Signaling mechanisms regulating endothelial permeability. Physiol Rev. 2006; 86:279–367. [PubMed: 16371600]
44. Min HY, Kim MS, Jang DS, Park EJ, Seo EK, Lee SK. Suppression of lipopolysaccharide-stimulated inducible nitric oxide synthase (iNOS) expression by a novel humulene derivative in macrophage cells. Int Immunopharmacol. 2009; 9:844–849. [PubMed: 19298870]
45. Mrak RE, Griffin WS. Interleukin-1, neuroinflammation, and Alzheimer's disease. Neurobiology of aging. 2001; 22:903–908. [PubMed: 11754997]
46. Musch MW, Walsh-Reitz MM, Chang EB. Roles of ZO1, occludin, and actin in oxidant-induced barrier disruption. Am J Physiol Gastrointest Liver Physiol. 2006; 290:222–231.
47. Myojin K, Taguchi A, Umetani K, Fukushima K, Nishiura N, Matsuyama T, Kimura H, Stern DM, Imai Y, Mori H. Visualization of intracerebral arteries by synchrotron radiation microangiography. AJNR Am J Neuroradiol. 2007; 28:953–957. [PubMed: 17494677]
48. Obeid R, McCaddon A, Herrmann W. The role of hyperhomocysteinemia and B-vitamin deficiency in neurological and psychiatric diseases. Clin Chem Lab Med. 2007; 45:1590–1606. [PubMed: 18067446]
49. Parnetti L, Palumbo B, Cardinali L, Loreti F, Chionne F, Cecchetti R, Senin U. Cerebrospinal fluid neuron-specific enolase in Alzheimer's disease and vascular dementia. Neuroscience letters. 1995; 183:43–45. [PubMed: 7746484]
50. Patibandla PK, Tyagi N, Dean WL, Tyagi SC, Roberts AM, Lominadze D. Fibrinogen induces alterations of endothelial cell tight junction proteins. J Cell Physiol. 2009; 221:195–203. [PubMed: 19507189]
51. Perna AF, Ingrosso D, De Santo NG. Homocysteine and oxidative stress. Amino Acids. 2003; 25:409–417. [PubMed: 14661100]
52. Petursdottir AL, Farr SA, Morley JE, Banks WA, Skuladottir GV. Lipid peroxidation in brain during aging in the senescence-accelerated mouse (SAM). Neurobiology of aging. 2007; 28:1170–1178. [PubMed: 16846666]
53. Rai S, Kamat PK, Nath C, Shukla R. A study on neuroinflammation and NMDA receptor function in STZ (ICV) induced memory impaired rats. Journal of neuroimmunology. 2013; 254:1–9. [PubMed: 23021418]
54. Rao JS, Kim HW, Kellom M, Greenstein D, Chen M, Kraft AD, Harry GJ, Rapoport SI, Basselin M. Increased neuroinflammatory and arachidonic acid cascade markers, and reduced synaptic proteins, in brain of HIV-1 transgenic rats. J Neuroinflammation. 2011; 8:101. [PubMed: 21846384]
55. Refsum H, Ueland PM, Nygard O, Vollset SE. Homocysteine and cardiovascular disease. Annual review of medicine. 1998; 49:31–62.
56. Romanic AM, White RF, Arleth AJ, Ohlstein EH, Barone FC. Matrix metalloproteinase expression increases after cerebral focal ischemia in rats: inhibition of matrix metalloproteinase-9 reduces infarct size. Stroke. 1998; 29:1020–1030. [PubMed: 9596253]
57. Rossoni G, Manfredi B, Razzetti R, Civelli M, Berti F. Positive interaction of the novel beta2-agonist carmoterol and tiotropium bromide in the control of airway changes induced by different challenges in guinea-pigs. Pulmonary pharmacology & therapeutics. 2007; 20:250–257. [PubMed: 16533614]
58. Schmued LC, Stowers CC, Scallet AC, Xu L. Fluoro-Jade C results in ultra-high resolution and contrast labeling of degenerating neurons. Brain research. 2005; 1035:24–31. [PubMed: 15713273]
59. Singh S, Gupta AK. Nitric oxide: role in tumour biology and iNOS/NO-based anticancer therapies. Cancer Chemother Pharmacol. 2011; 67:1211–1224. [PubMed: 21544630]

60. Stevenson BR, Siliciano JD, Mooseker MS, Goodenough DA. Identification of ZO1: a higher molecular weight polypeptide associated with the tight junction (zonula occludens) in a variety of epithelia. J Cell Biol. 1986; 103:755–766. [PubMed: 3528172]
61. Szabo C. Hydrogen sulphide and its therapeutic potential. Nature reviews Drug discovery. 2007; 6:917–935.
62. Tada Y, Yagi K, Kitazato KT, Tamura T, Kinouchi T, Shimada K, Matsushita N, Nakajima N, Satomi J, Kageji T, Nagahiro S. Reduction of endothelial tight junction proteins is related to cerebral aneurysm formation in rats. J Hypertens. 2010; 28:1883–1891. [PubMed: 20577123]
63. Takechi R, Pallebage-Gamarallage MM, Lam V, Giles C, Mamo JC. Aging-Related Changes in Blood-Brain Barrier Integrity and the Effect of Dietary Fat. Neurodegener Dis. 201210.1159/000343211
64. Tota S, Hanif K, Kamat PK, Najmi AK, Nath C. Role of central angiotensin receptors in scopolamine-induced impairment in memory, cerebral blood flow, and cholinergic function. Psychopharmacology (Berl). 2012; 222:185–202. [PubMed: 22362194]
65. Tsukita S, Furose M. Pores in the wall: claudins constitute tight junction strands containing aqueous pores. J Cell Biol. 2000; 149:13–16. [PubMed: 10747082]
66. Tyagi N, Givvimani S, Qipshidze N, Kundu S, Kapoor S, Vacek JC, Tyagi SC. Hydrogen sulfide mitigates matrix metalloproteinase-9 activity and neurovascular permeability in hyperhomocysteinemic mice. Neurochem Int. 2010; 56:301–307. [PubMed: 19913585]
67. Tyagi N, Moshal KS, Sen U, Vacek TP, Kumar M, Hughes WM Jr, Kundu S, Tyagi SC. H2S protects against methionine-induced oxidative stress in brain endothelial cells. Antioxidants & redox signaling. 2009; 11:25–33. [PubMed: 18837652]
68. Tyagi N, Ovechkin AV, Lominadze D, Moshal KS, Tyagi SC. Mitochondrial mechanism of microvascular endothelial cells apoptosis in hyperhomocysteinemia. J Cell Biochem. 2006; 98:1150–1162. [PubMed: 16514665]
69. Uttara B, Singh AV, Zamboni P, Mahajan RT. Oxidative stress and neurodegenerative diseases: a review of upstream and downstream antioxidant therapeutic options. Current neuropharmacology. 2009; 7:65–74. [PubMed: 19721819]
70. Weiss N, Papatheodorou L, Morihara N, Hilge R, Ide N. Aged garlic extract restores nitric oxide bioavailability in cultured human endothelial cells even under conditions of homocysteine elevation. Journal of ethnopharmacology. 2013; 145:162–167. [PubMed: 23127645]
71. White AR, Huang X, Jobling MF, Barrow CJ, Beyreuther K, Masters CL, Bush AI, Cappai R. Homocysteine potentiates copper- and amyloid beta peptide-mediated toxicity in primary neuronal cultures: possible risk factors in the Alzheimer's-type neurodegenerative pathways. Journal of neurochemistry. 2001; 76:1509–1520. [PubMed: 11238735]
72. Williams WM, Chung YW. Evidence for an age-related attenuation of cerebral microvascular antioxidant response to oxidative stress. Life Sci. 2006; 79:1638–1644. [PubMed: 16815478]
73. Wolf RC, Vasic N, Sambataro F, Hose A, Frasch K, Schmid M, Walter H. Temporally anticorrelated brain networks during working memory performance reveal aberrant prefrontal and hippocampal connectivity in patients with schizophrenia. Prog Neuropsychopharmacol Biol Psychiatry. 2009; 33:1464–1473. [PubMed: 19666074]
74. Yan SK, Chang T, Wang H, Wu L, Wang R, Meng QH. Effects of hydrogen sulfide on homocysteine-induced oxidative stress in vascular smooth muscle cells. Biochemical and biophysical research communications. 2006; 351:485–491. [PubMed: 17069760]
75. Zalev AH. Venous barium embolization, a rare, potentially fatal complication of barium enema: 2 case reports. Canadian Association of Radiologists journal = Journal l'Association canadienne des radiologistes. 1997; 48:323–326.
76. Zhao SP, Liu L, Gao M, Zhou QC, Li YL, Xia B. Impairment of endothelial function after a high-fat meal in patients with coronary artery disease. Coron Artery Dis. 2001; 12:561–565. [PubMed: 11714996]
77. Zhao Y, Wang H, Xian M. Cysteine-activated hydrogen sulfide (H2S) donors. J Am Chem Soc. 2011; 133:15–17. [PubMed: 21142018]
78. Zlokovic BV. The blood-brain barrier in health and chronic neurodegenerative disorders. Neuron. 2008; 57:178–201. [PubMed: 18215617]

Highlights

- Hcy (IC) induces Neurodegeneration along with memory impairment in mice.
- Oxidative stress and neuroinflammation stimulates cerebrovascular remodeling.
- MMPs and tight junction proteins are altered in Hcy (IC) treated mice brains.
- H_2S proved effective in Hcy induced neurotoxicity and cerebrovascular dysfunction.

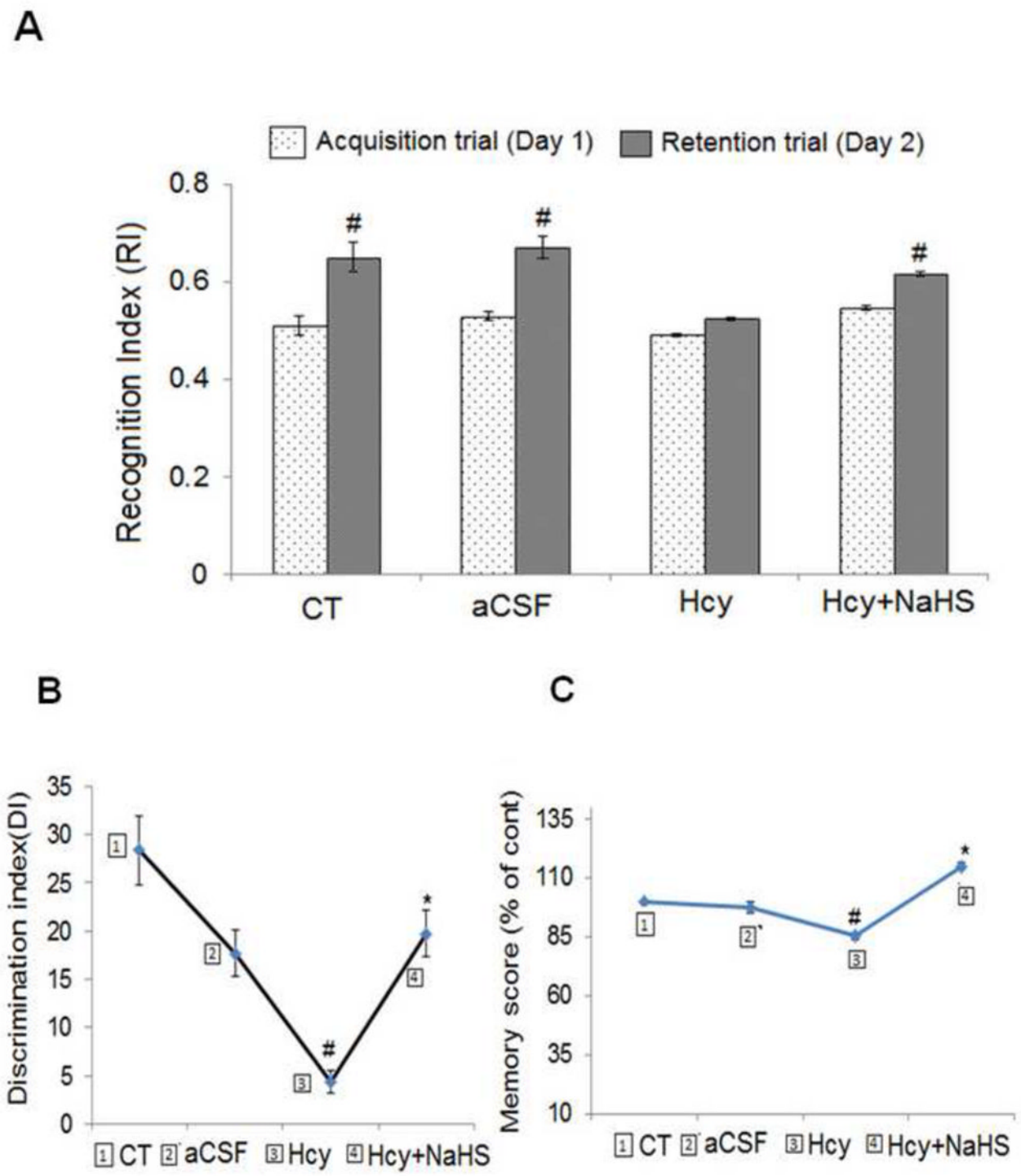

Fig. 1. Hcy (IC) induced memory impairment in mice

Mice were subjected to novel object recognition test. Results were expressed as, recognition index (Fig. 1A), discrimination index (Fig. 1B) and mean memory score (Fig. 1C). Data were analyzed by one-way ANOVA followed by Tukey's test for multiple comparisons.

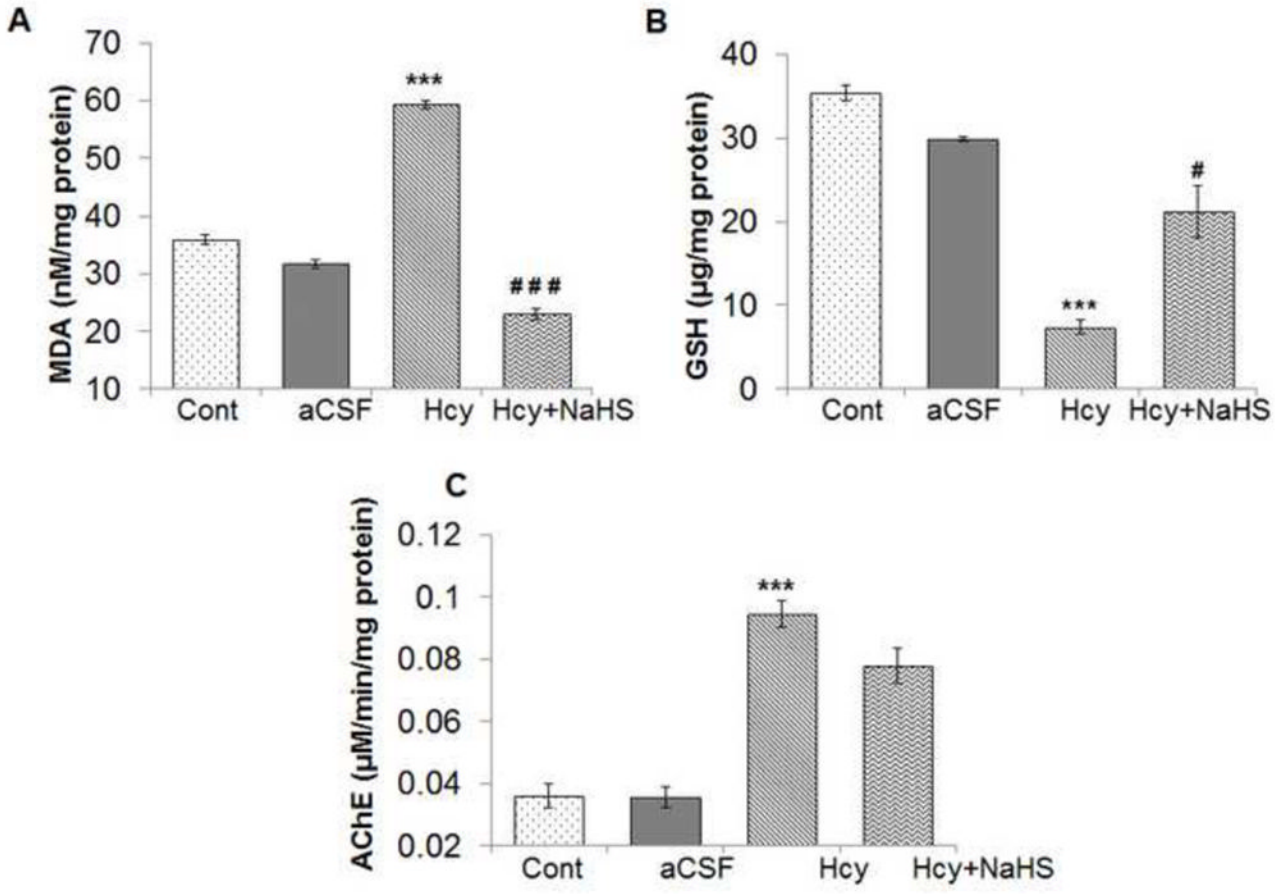

Fig. 2. Effect of NaHS on Hcy-induced alterations in malondialdehyde, intracellular reduced glutathione (GSH) and AChE levels

(A) MDA: [F(3, 16)=1.23; $P< 0.001$] **(B)** GSH: [F(3, 16)=2.2; $P< 0.005$] and **(C)** AChE: [F(3, 16)=1.2; $P< 0.01$] denotes Hcy significantly increased oxidative stress. A significant protection was observed with NaHS treatment. Data represents mean ±SE from n = 5 per group; $^{***}P< 0.0001$ *vs* control group, $^{\#}P< 0.05$, $^{\#\#\#}P< 0.0001$ *vs* to Hcy treated group.

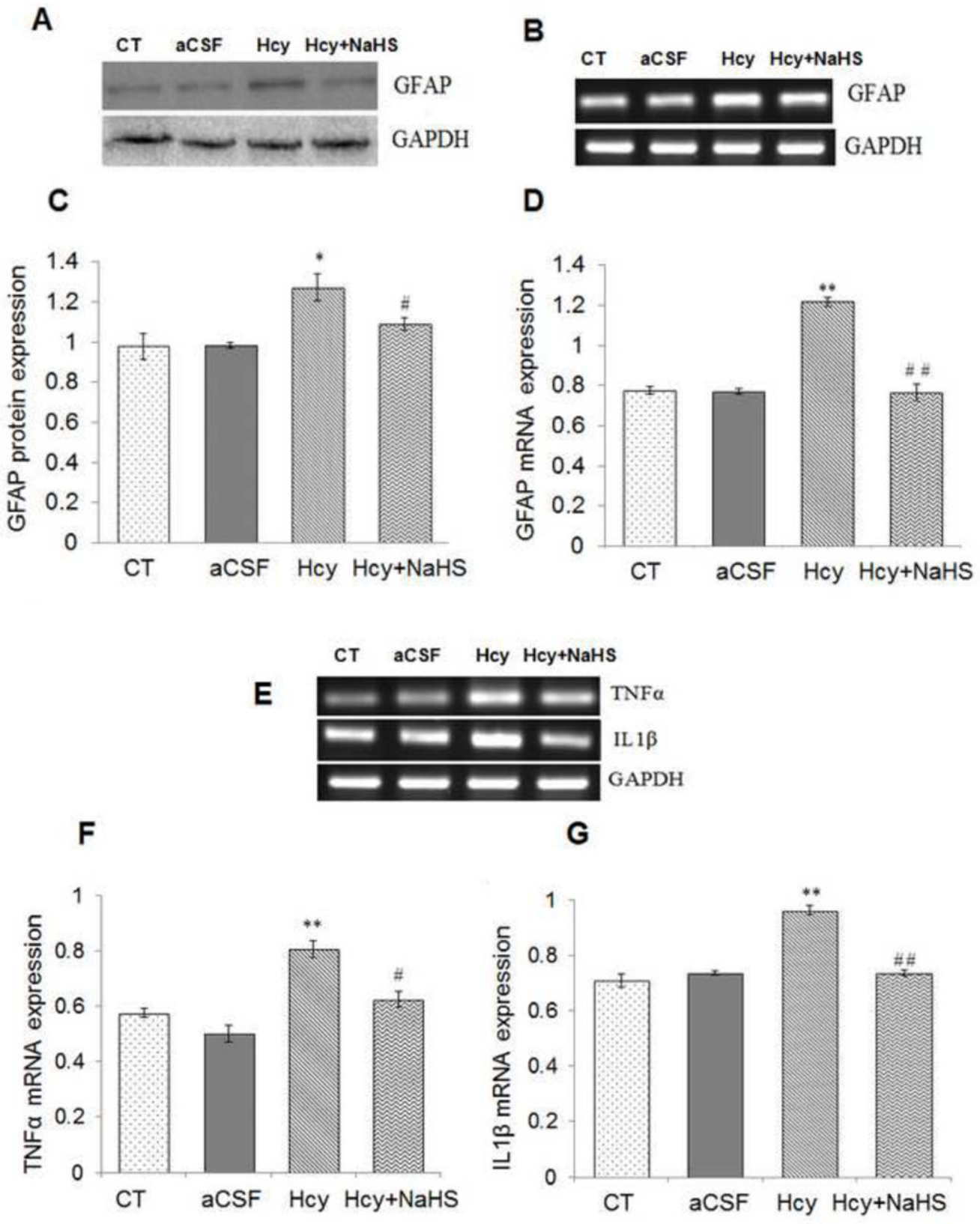

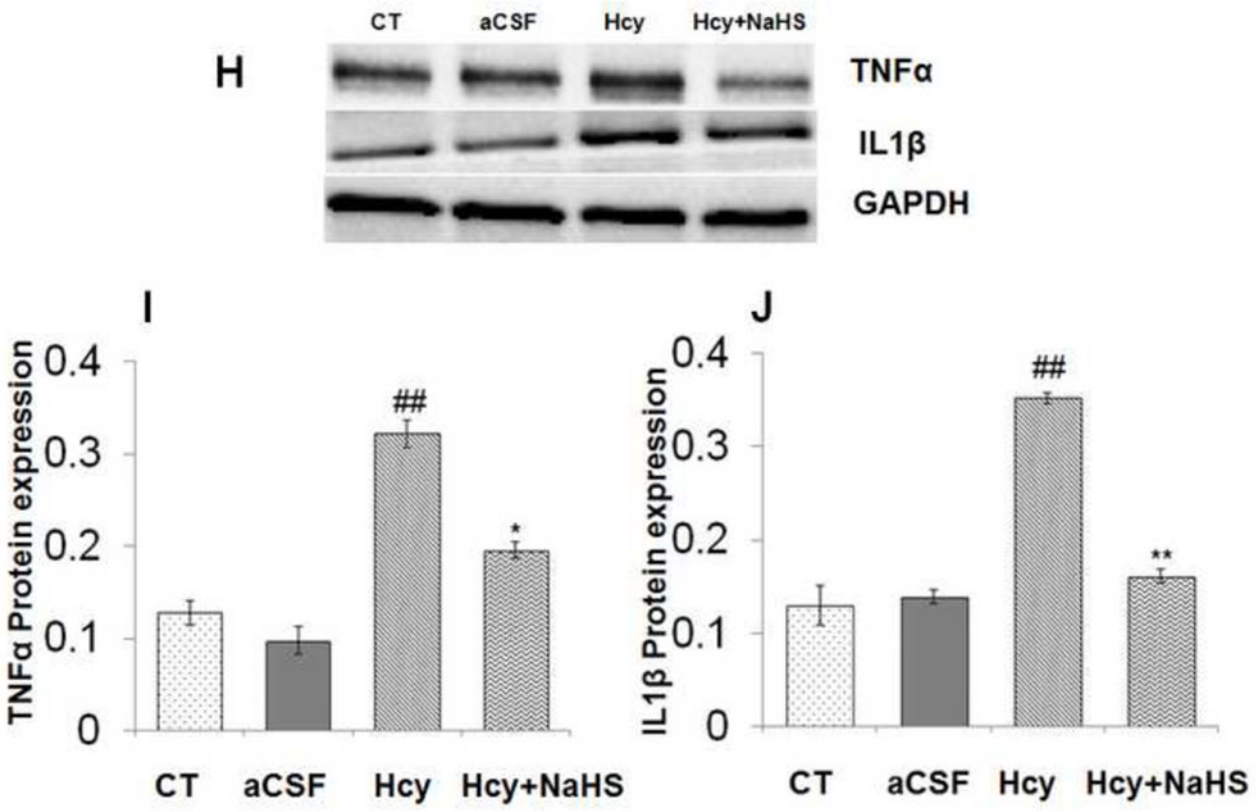

Fig. 3. Effect of NaHS on Hcy induced change in GFAP, TNFα and IL1β

(A) Western blot analyses of GFAP protein expression; [F(3, 16)=.93: $P< 0.005$] **(B)** RT-PCR analysis GFAP mRNA expression: [F(3, 16)=1.22; $P< 0.01$] in WT, WT+aCSF, WT +Hcy and Hcy-treated WT+NaHS mouse brain. The GAPDH was using as a loading control **(C& D)** Densitometry analysis of GFAP protein/mRNA expressions as represented in the bar diagram. **(E)** Western blot analyses of TNFα protein expression: [F(3, 16)=1.93; $P< 0.01$] and IL1β: [F(3, 16)=.73; $P< 0.01$]. **(F)** RT-PCR analysis TNFα: [F(3, 16)=.22; $P< 0.005$] and IL1β mRNA expression: [F(3, 16)=.72; $P< 0.001$]. The GAPDH was using as a loading control **(G& H)** Densitometry analysis of TNFα and IL1β protein/mRNA expressions as represented in the bar diagram. Data represents mean ±SE from n = 5 per group. $^{*}P< 0.05$, $^{**}P< 0.005$ *vs* Control group and $^{\#}P< 0.05$, $^{\#\#}P< 0.001$ *vs* Hcy treated group.

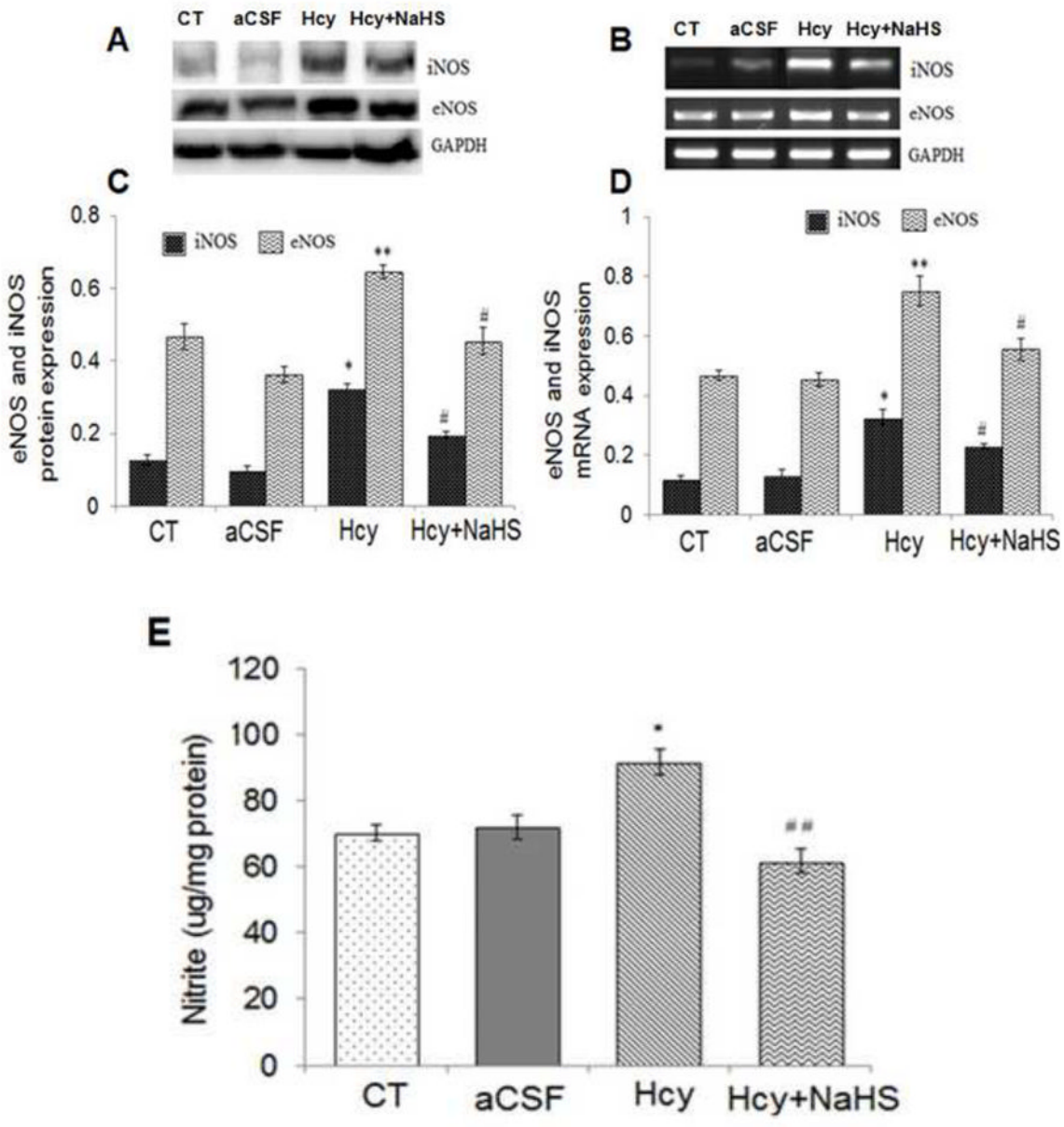

Fig. 4. Effect of NaHS on nitric oxide bioavailability

(A) Western blots analyses of eNOS: [F(3, 16)=1.23; $P< 0.01$] and iNOS protein: [F(3, 16)=1.5; $P< 0.01$] **(B)** RT-PCR analysis of eNOS: [F(3, 16)=2.21; $P< 0.005$] and iNOS mRNA expression: [F(3, 16)=1.13; $P< 0.01$] in WT, WT+aCSF, WT+Hcy and Hcy-treated WT+NaHS mouse brain. The GAPDH was using as a loading control **(C&D)** Densitometry analysis of eNOS and iNOS protein/mRNA expressions as represented in the bar diagram. **(E)** Nitrite: [F(3, 16)=2.23; $P< 0.05$]. Data represents mean ±SE from n = 5 per group. $^{*}P< 0.05$, $^{**}P< 0.005$ *vs* Control group and $^{\#}P< 0.05$, $^{\#\#}P< 0.001$ *vs* Hcy treated group

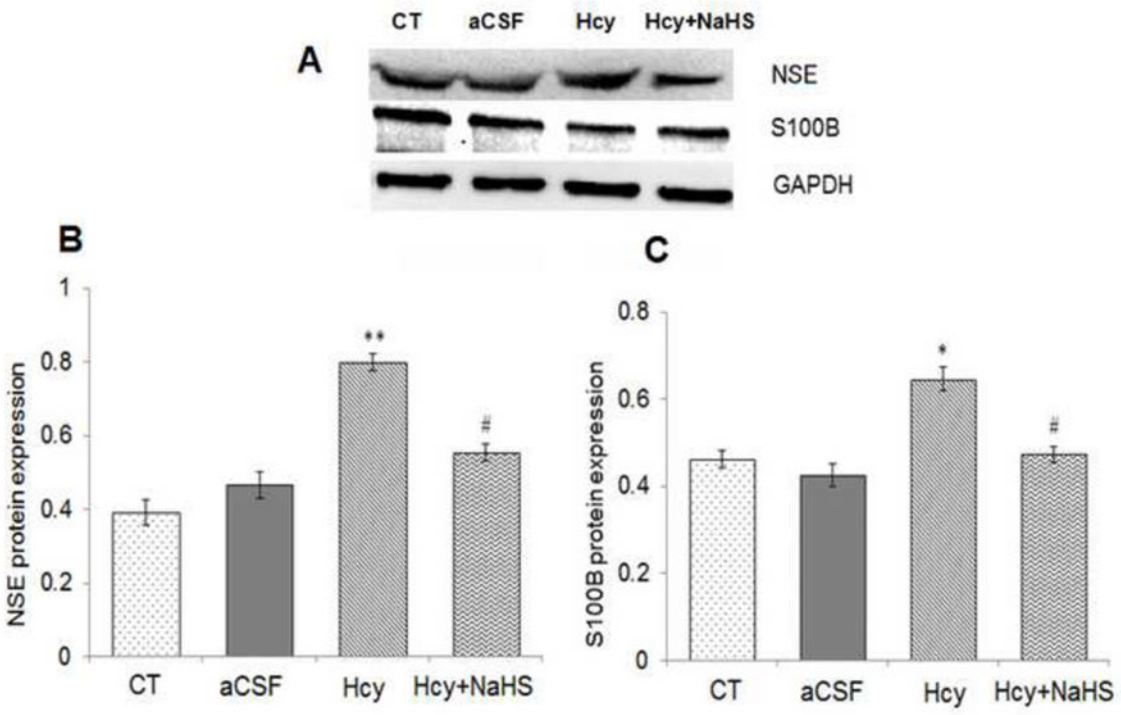

Fig. 5. Effect of NaHS on neuronal damage markers

(A) Western blots analyses of S100 calcium-binding protein B (S100B): [F(3, 16)=.81; $P<$ 0.01] and neuron-specific enolase (NSE): [F(3, 16)=.33: $P<$ 0.01] in mouse brain. The GAPDH was using as a loading control (**B& C)** Densitometry analysis of S100B and NSE protein expressions as represented in the bar diagram. Data represents mean ±SE from n = 5 per group. $^{*}P< 0.05$, $^{**}P< 0.005$ *vs* Control group and $^{\#}P< 0.05$, $^{\#\#}P< 0.001$ *vs* Hcy treated group.

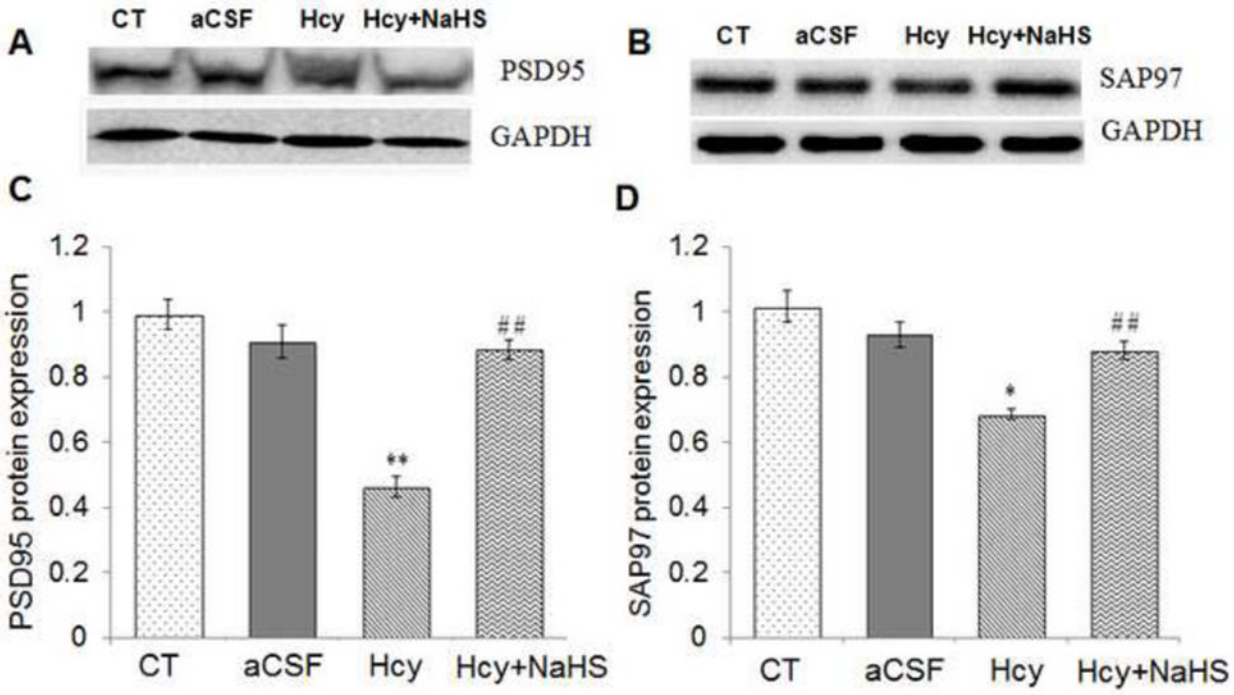

Fig. 6. Effect of NaHS on synaptic proteins

(A) Western blots analyses of PSD95: [F(3, 16)=.61; $P< 0.01$] (**B)** SAP97protein expression: [F(3, 16)=.83; $P< 0.05$] in different treated groups. The GAPDH was using as a loading control (**B& C)** Densitometry analysis of PSD95 and SAP97 protein expressions as represented in the bar diagram. Data represents mean ±SE from n = 5 per group. $^{*}P< 0.05$, $^{**}P< 0.005$ *vs* Control group and $^{\#}P< 0.05$, $^{\#\#}P< 0.001$ *vs* Hcy treated group.

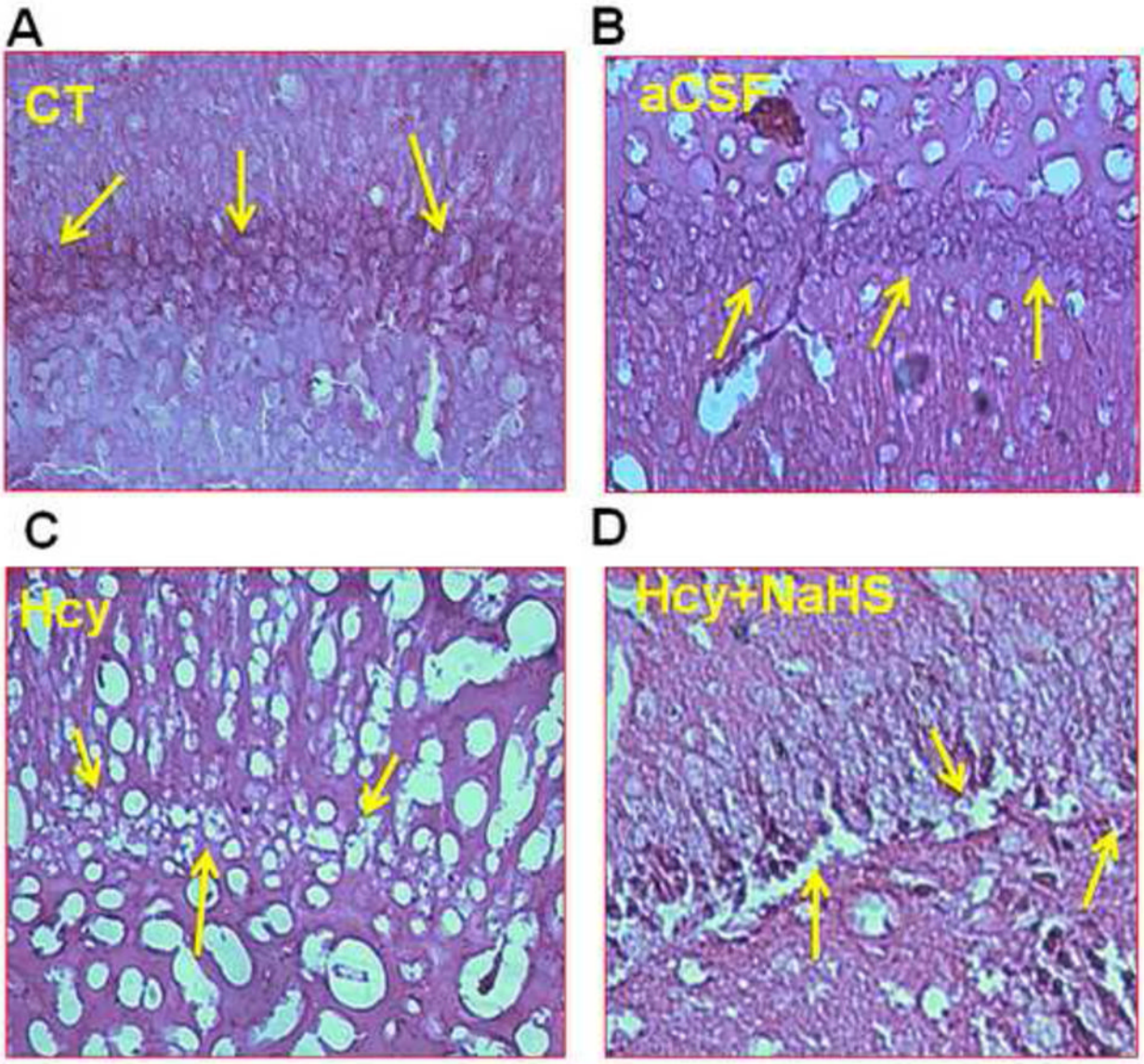

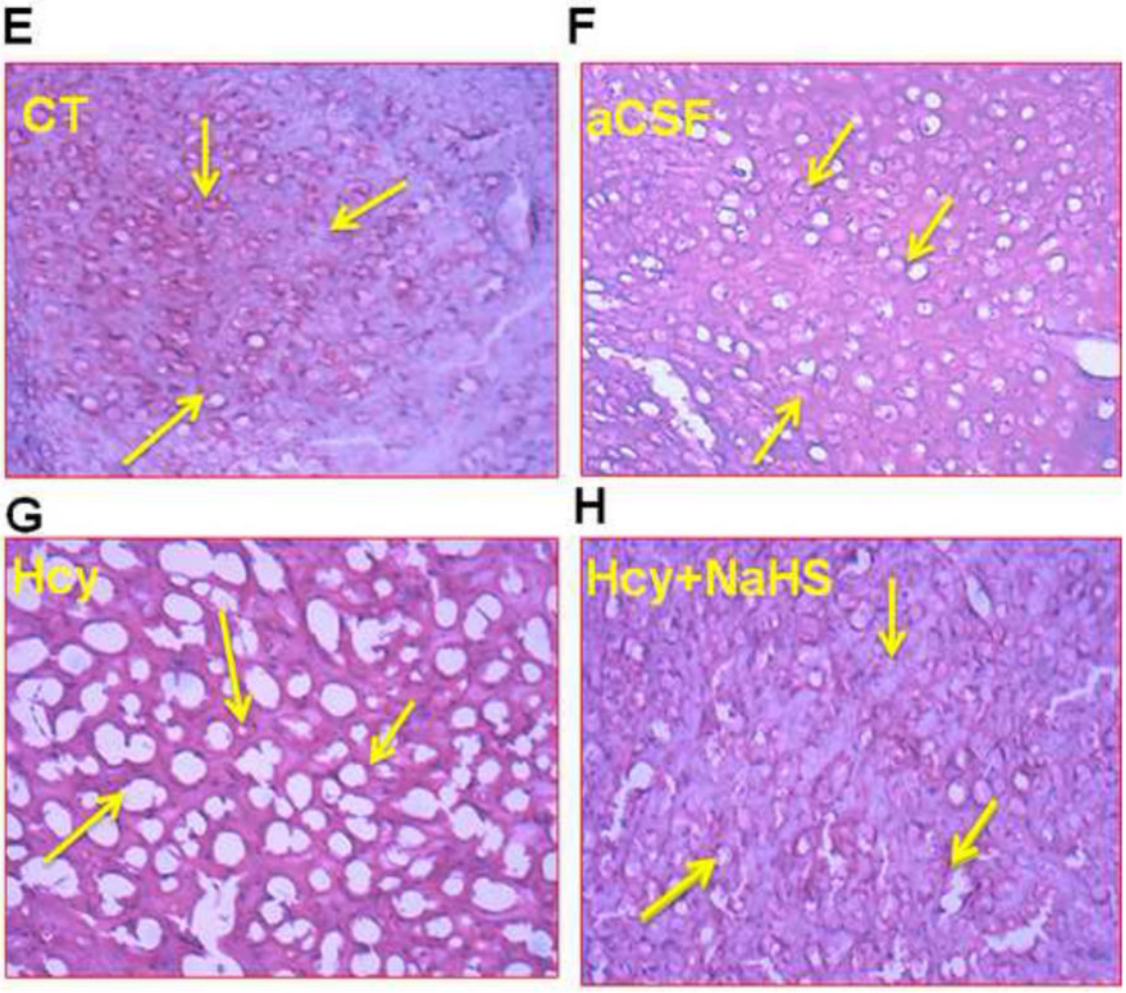

Fig. 7. Hematoxylin and eosin (H&E) staining in frozen brain sections in WT, WT+aCSF, WT +Hcy and Hcy-treated WT+NaHS groups

(A) Representative picture of control hippocampus region **(B)** aCSF did not reveal difference in cell numbers in the neurons of hippocampus region **(C)** Death of the neurons of hippocampus region revealed degeneration in the hippocampus of Hcy-treated mice **(D)** Less degeneration is observed in hippocampus region of NaHS treated group. While in periventricular cortex **(E)** control **(F)** aCSF did not reveal difference in cortical cells while **(G)** Hcy administration showed remarkable degeneration (sponginess of the cell) of periventricular cortical neurons **(H)** NaHS treatment showed less periventricular cortex neuronal degeneration than Hcy treated mice as indicated by arrows (sponginess, condensed nucleus) at 60x magnification. Note: Arrow is showing periventricular cortex neuronal degeneration area.

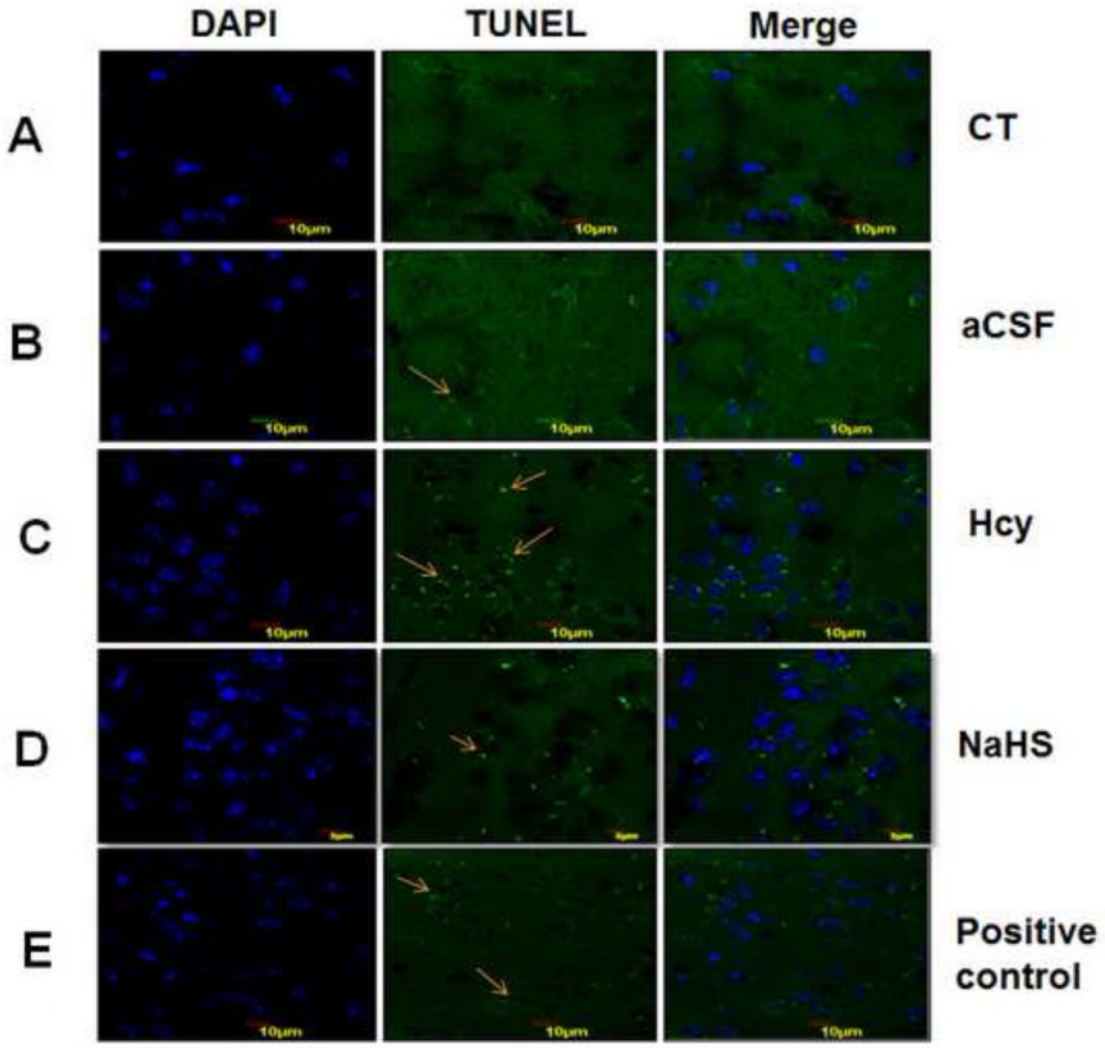

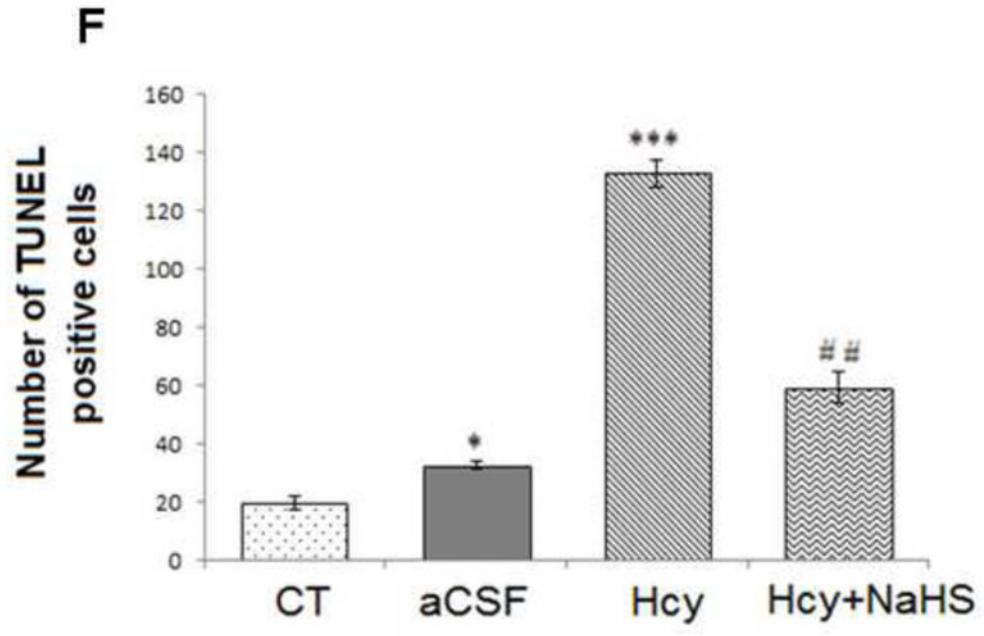

Fig. 8. Tunnel assay for apoptosis in WT, WT+aCSF, WT+Hcy and Hcy-treated WT+NaHS groups

Apoptotic cells are seen as green fluorescent dots (scale bar- 10 μm). No difference observed in apoptotic cells of control **(A)** and CSF **(B)** group. Apoptotic cell death was increased in Hcy treated brain **(C).** NaHS treament decreased the apoptotic cell **(D).** Positive control also represented in this image **(E).** Bar graph representing a significance of difference between different treatment groups **(F).** Data represents mean ±SE from n = 5 per group; $^{*}P< 0.05$, $^{**}P< 0.005$ *vs* Control group and $^{\#}P< 0.05$, $^{\#\#}P< 0.001$ *vs* Hcy treated group. Note: Arrow is showing apoptotic cells.

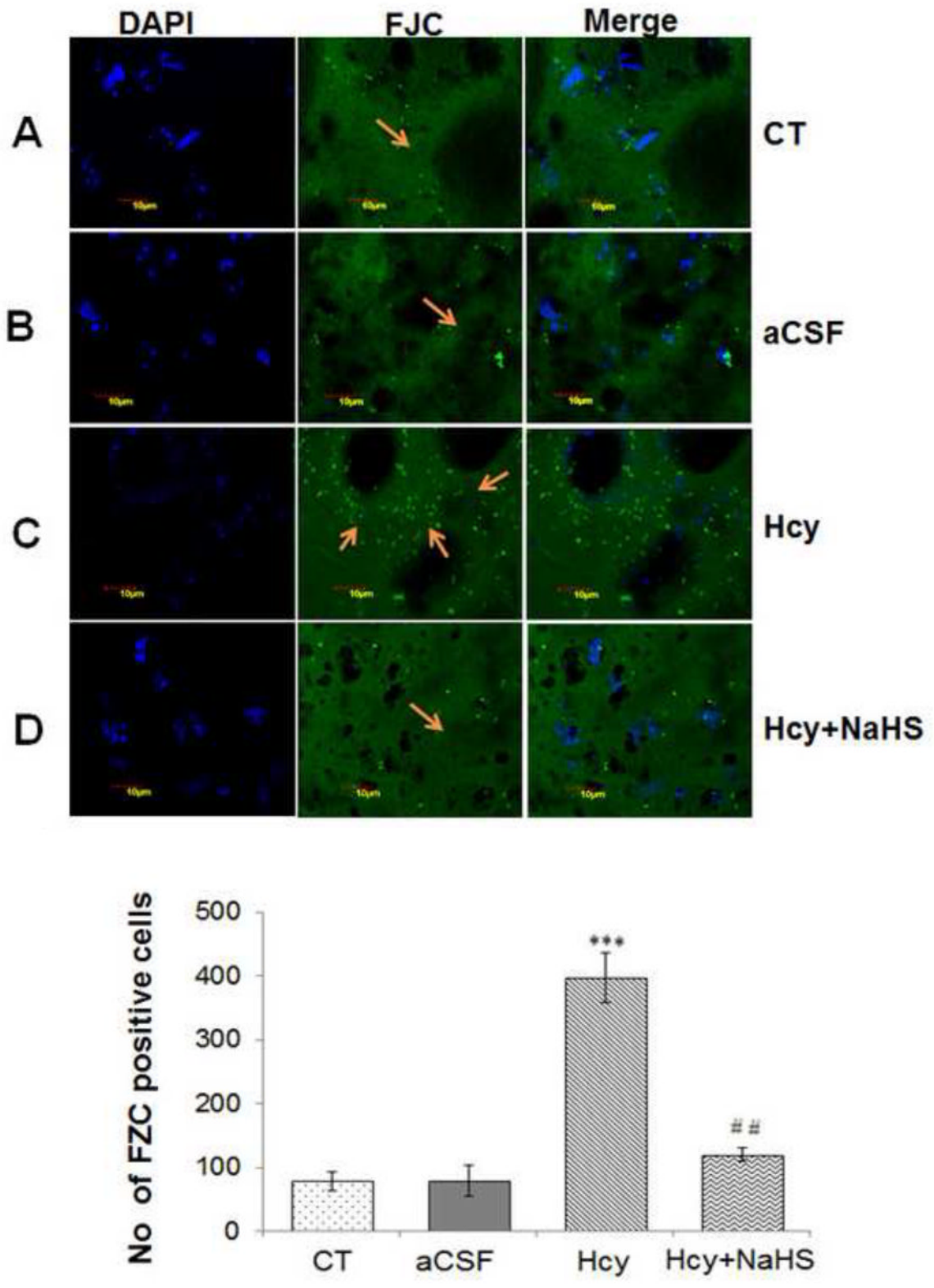

Fig. 9. Representative Photomicrographs of fluro Jade-C (FJC) staining

(A) Control (**B)** aCSF did not reveal difference in FJC positive cells **(C)** A significant increase in FJC positive cell indicates degeneration of neuronal cells in Hcy-treated mice. A significant less numbers of FJC positive cells are observed in NaHS **(D)** treated mice indicates neuro-protective effect of H2S. Fig. E represents the bar diagram of FJC positive cell (expressed in arbitrary unit). $^{***}P< 0.0001$ *vs* Control group and $^{\#\#}P< 0.005$, *vs* Hcy treated group. Note: Arrow is showing degenerating neurons.

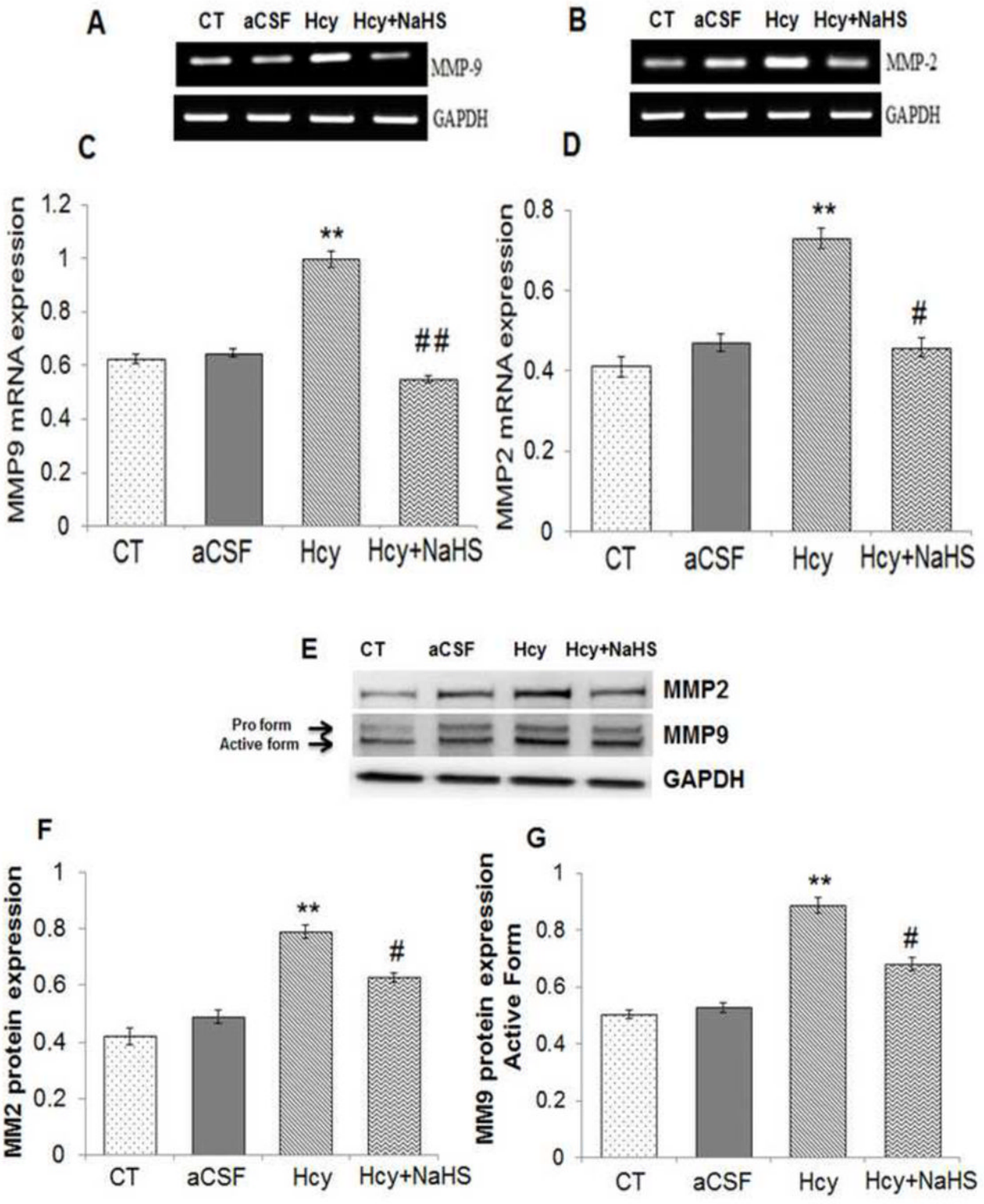

Fig. 10. Effect of NaHS on MMPs

(A) RT-PCR analysis of MMP-9 mRNA expression: [F(3, 16)=1.29; $P< 0.01$] **(B)** RT-PCR analysis of MMP-2 mRNA expression [F(3, 16)=1.33; $P< 0.001$] in WT, WT+aCSF, WT +Hcy and Hcy-treated WT+NaHS mouse brain. The GAPDH was using as loading control **(C&D)** Densitometry analysis of MMP-9 and MMP-2 mRNA expressions as represented in the bar diagram. Data represents mean ±SE from n = 5 per group. $^{**}P< 0.005$ *vs* Control group *and* $^{\#}P< 0.01$, *vs* Hcy treated group.

(E) Western blot analysis of MMP-2: [F(3, 16)=1.1; $P< 0.001$] and MMP-9: [F(3, 16)=.76; $P< 0.001$] protein expression in different treated groups. The GAPDH was using as loading control **(F&G)** Densitometry analysis of MMP-2/MMP-9 protein expressions as represented in the bar diagram. Data represents mean ±SE from n = 5 per group. $^{**}P< 0.005$ *vs* Control group and $^{\#}P< 0.01$, *vs* Hcy treated group.

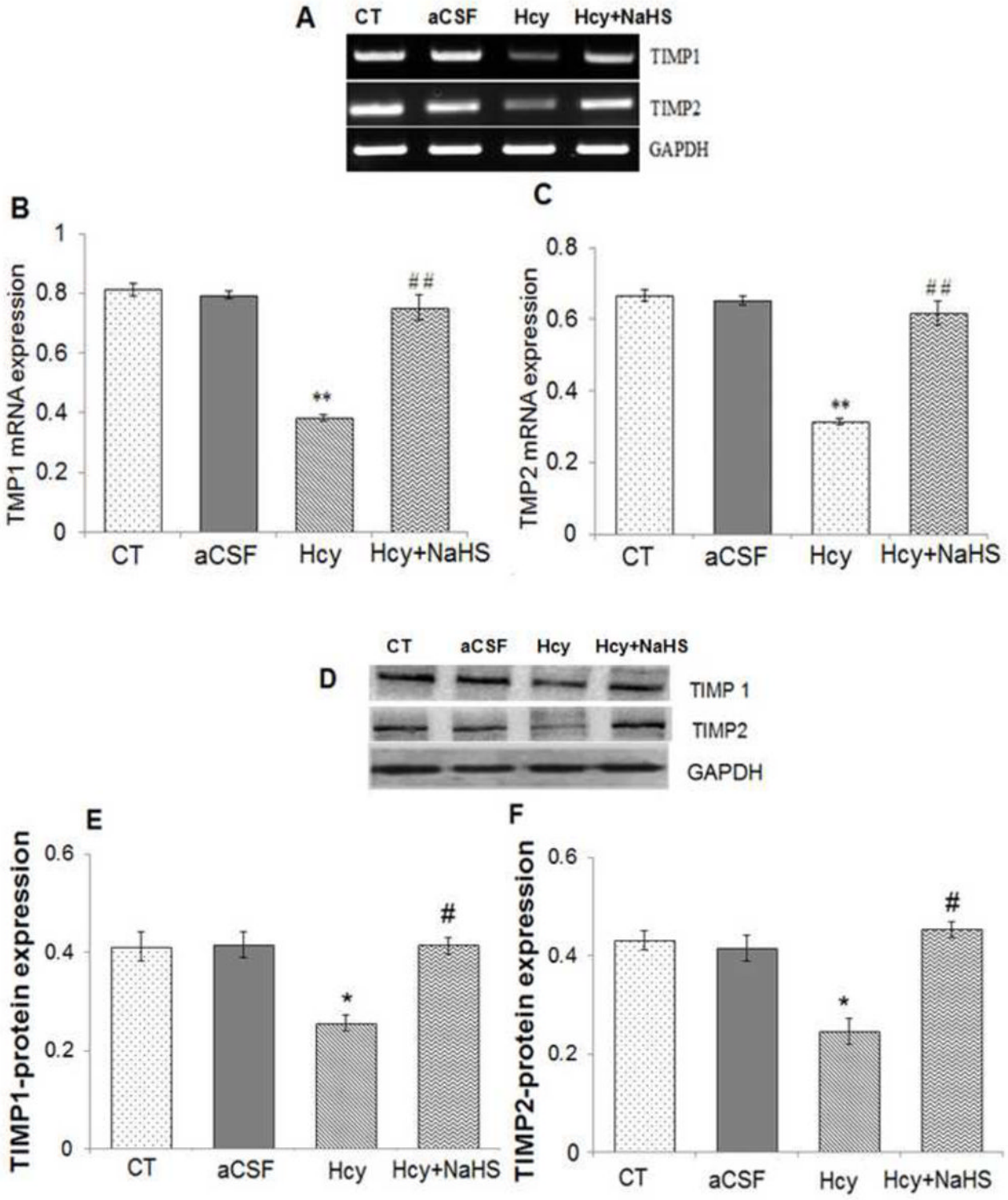

Fig. 11. Effect of NaHS on TIMPs

(A) RT-PCR analysis of TIMP-1: [F(3, 16)=1.45; $P< 0.005$] and TIMP-2 mRNA expression: [F(3, 16)=.63; $P< 0.01$] in WT, WT+aCSF, WT+Hcy and Hcy-treated WT +NaHS mouse brain. The GAPDH was using as loading control **(B&C)** Densitometry

analysis of TIMP-1/TIMP-2 mRNA expressions as represented in the bar diagram. Data represents mean ±SE from n = 5 per group. $^{**}P< 0.005$ *vs* Control group and $^{\#\#}P< 0.001$ vs Hcy treated group.

(D) Western blot analysis of TIMP-1: [F(3, 16)=.34; $P< 0.001$] and TIMP-2: [F(3, 16)=.55; $P< 0.05$] protein expression in mouse brain. The GAPDH was using as loading control **(E & F)** Densitometry analysis of TIMP-1/TIMP-2 protein expressions as represented in the bar diagram. Data represents mean ±SE from n = 5 per group. $^{**}P< 0.005$ *vs* Control group and $^{\#}P< 0.01$, $^{\#\#}P< 0.001$ *vs* Hcy treated group.

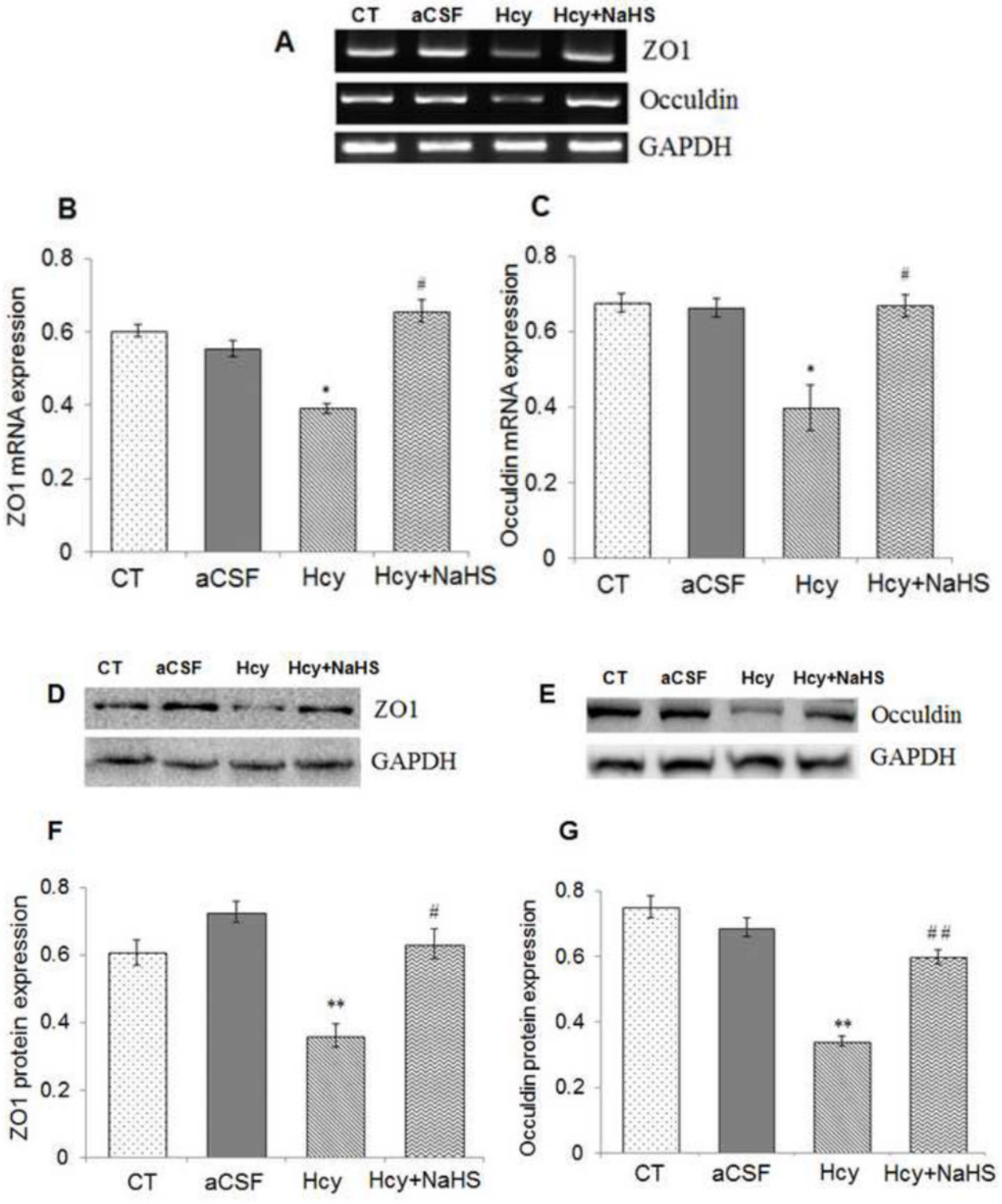

Fig. 12. Effect of NaHS on Hcy-induced alterations in tight junction proteins

(A) RT-PCR analysis of ZO-1: [F(3, 16)=.97; *P*< 0.001] and Occuldin: [F(3, 16)=1.23; *P*< 0.01] mRNA expression in different treatment groups. The GAPDH was using as loading control **(B&C)** Densitometry analysis of ZO-1 and Occuldin mRNA expressions as

represented in the bar graph **(D, E)** Western blot analysis of ZO-1: [F(3, 16)=.59; $P< 0.001$] and Occuldin: [F(3, 16)=.23; $P< 0.001$] protein expression in WT, WT+aCSF, WT+Hcy and Hcy-treated WT+NaHS mouse brain. Densitometry analysis of ZO-1 and Occuldin protein expressions as represented in the bar diagram **(F &G)**. Data represents mean ±SE from n = 4 per group. $^{**}P< 0.005$ *vs* Control group, $^{\#}P< 0.01$, $^{\#\#}P< 0.005$ *vs* Hcy treated group.

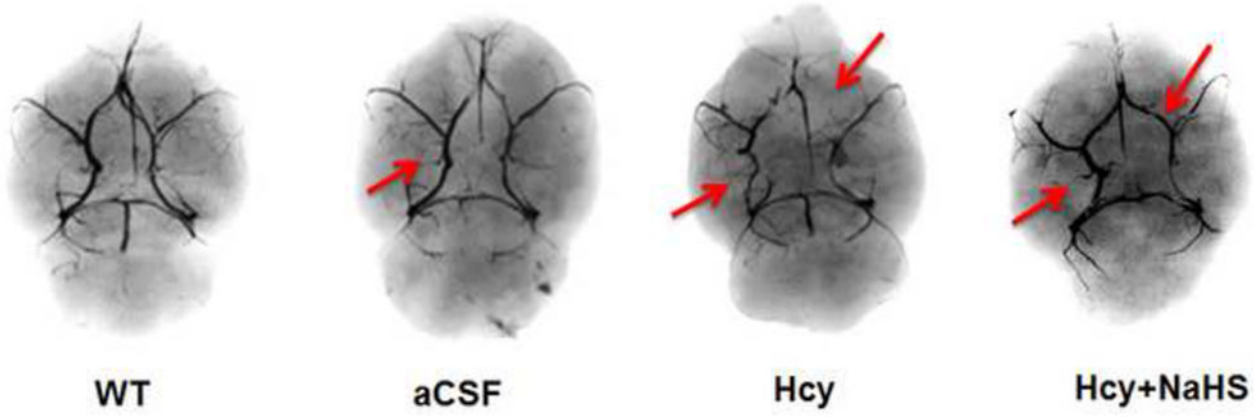

Fig. 13.
Brain angiography Study in mice brain showed the loss of major vessel in Hcy treated mice brain which was recovered by NaHS treatment. Note: Arrow showing major blood vessel.

Table 1

Representative Table is showing the primer of different gene

Genes	Orientation	Primers sequences
MMP9	Forward Primers Reverse Primers	5′-AAGGCAAACCCTGTGTGTTC-3′ 5′-GTGGTTCAGTT GTGGTGGTG-3′
MMP2	Forward Primers Reverse Primers	5′-GCACTCTGGAGCGAGGATAC -3′ 5′-GCCCTCCTAAGCCAGTCTCT-3′
iNOS	Forward Primers Reverse Primers	5′-AACGGAGAACGTTGGATTTG-3′ 5′-CAGCACAAGGGGTTTTCTTC-3′
eNOS	Forward Primers Reverse Primers	5′-CTGTGGTCTGGTGCTGGTC-3′ 5′-TGGGCAACTTGAAGAGTGTG-3′
ZO-1	Forward Primers Reverse Primers	5′-AAGGCAATTCCGTATCGTTG-3′ 5′-CCACAGCTGAAGGACTCACA-3′
Occuldin	Forward Primers Reverse Primers	5′-GAGGGTACACAGACCCCAGA-3′ 5′-CAGGATTGCGCTGACTATGA-3′
TIMP1	Forward Primers Reverse Primers	5′-ACCATGGCCCCCTTTGAGCCCCTG-3′ 5′-TCAGGCTATCTGGGACCGCAGGGA-3′
TIMP2	Forward Primers Reverse Primers	5′-CTCGGCAGTGTGTGGGGTC-3′ 5′-CGAGAAACTCCTGCTTGGGG-3′
GFAP	Forward Primers Reverse Primers	5′-CGAGTCCCTAGAGCGGCAAATG-3′ 5′-CGGATCTGGAGGTTGGAGAAAGTC-3′
TNFα	Forward Primers Reverse Primers	5′-CCAGGAGAAAGTCAGCCTCCT-3′ 5′-TCATACCAGGGCTTGAGCTCA-3′
IL1-β	Forward Primers Reverse Primers	5′-CACCTCTCAAGCAGAGCACAG-3′ 5′-GGGTTCCATGGTGAAGTCAAC-3′
GAPDH	Forward Primers Reverse Primers	5′-TGAAGGTCGGTGTGAACGGATTTGGC-3′ 5′-CATGTAGGCCATGAGGTCCACCAC-3′